GRANT/LEWIS

107 pages

GAS TURBINE LABORATORY
DEPARTMENT OF AERONAUTICS AND ASTRONAUTICS
MASSACHUSETTS INSTITUTE OF TECHNOLOGY
CAMBRIDGE, MA 02139

IN-18362

A FINAL REPORT ON

NASA GRANT NAG-3-697

entitled

A SUPERSONIC FAN EQUIPPED VARIABLE CYCLE ENGINE FOR A MACH 2.7 SUPERSONIC TRANSPORT

by

T.S. Tavares

prepared for

NASA Lewis Research Center
Cleveland, OH 44135

August 22, 1985

A SUPERSONIC FAN EQUIPPED VARIABLE CYCLE ENGINE FOR A MACH 2.7 SUPERSONIC TRANSPORT

by

Theodore Sean Tavares

A SUPERSONIC FAN EQUIPPED VARIABLE CYCLE ENGINE

FOR A MACH 2.7 SUPERSONIC TRANSPORT

by

THEODORE SEAN TAVARES

ABSTRACT

A design study was carried out to evaluate the concept of a variable cycle turbofan engine with an axially supersonic fan stage as powerplant for a Mach 2.7 supersonic transport. The study comprises two parts; a propulsion system study and a design of blade cascades for the fan stage.

In performing the system study, quantitative cycle analysis was used to assess the effects of the fan inlet and blading efficiencies on engine performance. Thrust levels predicted by cycle analysis are shown to match the thrust requirements of a representative aircraft. Fan inlet geometry is discussed and it is shown that a fixed geometry conical spike will provide sufficient airflow throughout the operating regime.

The supersonic fan considered in this study consists of a single stage comprising a rotor and stator. The concept is similar in principle to a supersonic compressor, but differs by having a stator which removes swirl from the flow without producing a net rise in static pressure.

In the chapter on blading design, operating conditions peculiar to the axially supersonic fan are discussed. Geometry of rotor and stator cascades are presented which utilize a supersonic vortex flow distribution. Results of a 2-D CFD flow analysis of these cascades are presented. A simple estimate of passage losses was made using empirical methods.

TABLE OF CONTENTS

LIST OF FIGURES

TABLES

1. INTRODUCTION

A design study was performed on the concept of a turbofan engine for a Mach 2.7 Supersonic Transport which employs a fan stage designed to operate with a supersonic axial component of the flow at the fan face. The study comprises two parts. Chapter 2 reports results of a system study, the main objective of which was to assess the effects of efficiency of the fan stage and its inlet on engine cycle performance and to identify characteristics of a suitable fan inlet. Chapter 3 presents candidate fan geometries, discusses operating conditions unique to such a fan, and presents results of a computational flow analysis of the blading.

1.1 BACKGROUND

Since 1972 NASA has sponsored studies to identify propulsion concepts suitable for long range supersonic cruise aircraft. These studies considered a number of conventional and variable cycle concepts. One alternative, the variable cycle engine with supersonic throughflow fan was proposed by Dr. Antonio Ferri and studied by Advanced Technology Laboratories (Ref. 1). Further work on the concept was carried out by investigators at NASA-Lewis (Ref. 2). The results of these studies showed that these so-called superflow engines could provide substantial improvement in the mission capabilities of aircraft with long range supersonic cruise requirements.

When compared with mission results of aircraft powered with

engines more conventional in concept, the range capability of a baseline supersonic transport was increased by about 20 percent or 1000 nautical miles when powered by the superflow engine. The specific fuel consumption of the superflow engines were judged to be on the order of 12 percent lower. This was due in large part to lower inlet and nacelle losses for the superflow engine and more versatility in cycle variations.

Estimates of weight suggest a 30 percent reduction in installed weight for the superflow engine. For the more conventional concept engines, the inlet, nozzles, and nacelle make up about 50 percent of the propulsion system weight. The inlet systems for the superflow engines were estimated to be about 50 percent lighter than that of more conventional turbofans and additional weight savings result in that the superflow engine uses a single stage fan while the reference turbofan requires three stages.

Very little work has been performed on supersonic compressors or fans with supersonic axial velocity. The analysis of supersonic fan blading performed by Trucco in Reference 1 addresses the unique operational differences between the axially supersonic fan and older supersonic compressor concepts and predicts high efficiency for a supersonic fan. Some experimental work on an axially supersonic rotor was performed by Breugelmans (Ref. 11). This work is discussed further in Chapter 3.

1.2 DESCRIPTION OF CONCEPT

The supersonic fan discussed in this report is variously referred to as a supersonic throughflow or superflow fan. It is designed to be operated with the axial component of the flow at the fan face supersonic, and supersonic flow is maintained throughout the rotor and stator. At flight conditions where supersonic flow cannot be maintained at the fan face, the flow at this location is choked. Thus this stage always operates with the axial component of the flow at least sonic.

This type of fan is distinguished from others which may have supersonic relative flow over part of the fan, such as the transonic fans which operate with subsonic axial Mach numbers throughout, but in which the flow relative to the blades at the outer radii is supersonic. Other rotors referred to as being supersonic, throughout, but in which the axial component of the flow is subsonic should not be confused with that referred to in this study.

The variable bypass engine is shown schematically in Figure 1.1. Since the fan can accept axially supersonic flow, a simple spike inlet, providing only minimal diffusion can be used. The flow leaving the fan stage is split into two streams, one of which enters the core of the engine. The other stream enters the fan nozzle. The flow leaving the fan is always supersonic, and variable bypass features can be attained by movement of the flow splitter lip.

A variable geometry diffuser leading to the core decelerates

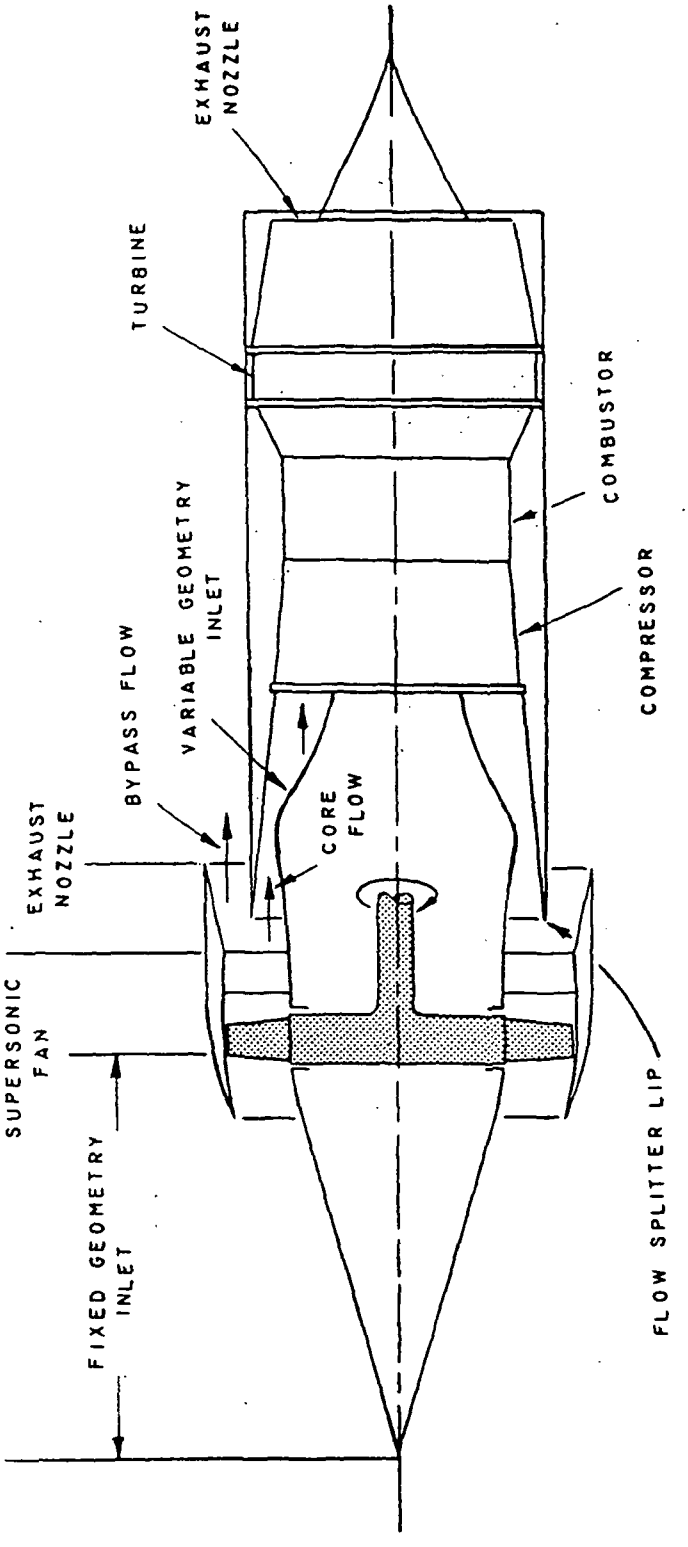

Figure 1.1 Schematic Drawing of Variable Bypass Supersonic Throughflow Turbofan

the flow to subsonic conditions, as required by the conventional (i.e. subsonic) gas generator. The fan exhaust nozzle has variable geometry to permit optimum expansion throughout the flight envelope.

The superflow fan selected for the present study has a design airflow of 1520 lb/sec at sea level static conditions. Its inlet is a conical spike, with a half angle of 16 degrees, and the system study performed herein suggests that it may be of fixed geometry and still provide adequate airflow throughout the flight envelope. Only slight diffusion of the bypass flow is carried out, from a free stream Mach number of 2.7 to Mach 2.2 at the fan face.

The supersonic fan is a single stage rotor-stator combination which generates thrust by increasing the velocity of the incoming flow without a static pressure rise across the stage. This implies that the Mach number at the fan exit is always higher than at the entrance, and hence always supersonic. This feature eliminates the need for a convergent-divergent section in the fan nozzle duct. The area of the fan nozzle is variable to permit expansion to ambient pressure.

The second inlet for the core flow has variable geometry. Fore and aft translation of its flow splitter lip may be used to vary the bypass ratio. (It may be one of the major technological challenges of this concept to achieve good performance of this component at all operating points.) As indicated previously, the gas generator is conventional in concept and is similar to that proposed in other more conventional propulsion concepts for long

range supersonic aircraft. A two spool turbine is utilized allowing some degree of independence between fan and core compressor to facilitate variable cycle features. The core flow exhaust nozzle has variable exit area for optimum expansion under a variety of operating conditions.

2. PROPULSION SYSTEM STUDY

One of the primary goals of the project was to work on the aerodynamic design of an axially supersonic fan stage. However, before proceeding with this task, it was felt prudent to perform a system study and compare expected engine performance with the requirements of a representative airframe. This would give some perspective as to the operational requirements of the fan.

The system study consists of two parts. A quantative cycle analysis was performed in which emphasis was placed on the effects of fan, diffuser, and core compressor efficiencies on engine performance. The fan inlet geometry was studied. The capture schedule of a conical spike inlet was compared to the capture schedule needed to meet airframe thrust constraints.

The following symbols are used in the system study:

π_d	Pressure ratio in diffusing from free stream to core compressor
π_d'	Pressure ratio in diffusing from free stream to fan face
π_b	Pressure ratio across burner
π_n'	Pressure ratio across fan nozzle
π_n	Pressure ratio across core nozzle
η_b	Burner efficiency
e_c	Polytropic efficiency in compression of core flow from diffuser exit to compressor exit
e_c'	Polytropic efficiency of fan
e_t	Polytropic efficiency of turbine
π_c	Compression ratio of core flow
π_c'	Compression ratio of fan flow
T_{t4}	Turbine inlet temperature
α	Bypass ratio
F	Thrust
p_∞	Ambient pressure
I_{sp}	Specific impulse
M_∞	Flight Mach number
A_{ff}	Flow area at fan face
A_{cowl}	Swept area of fan cowl
$A_{capture}$	Inlet capture streamtube area

2.1 MISSION PROFILE AND AIRFRAME THRUST REQUIREMENTS

2.1.1 MISSION PROFILE

The nominal mission studied was a Mach 2.7 cruise at 65,000 ft. A U.S. Standard Atmosphere was assumed. The climb and acceleration path used in this study is shown in terms of Altitude and Mach number in Figure 2.1. The relevant atmospheric characteristics are tabulated in Table 1.

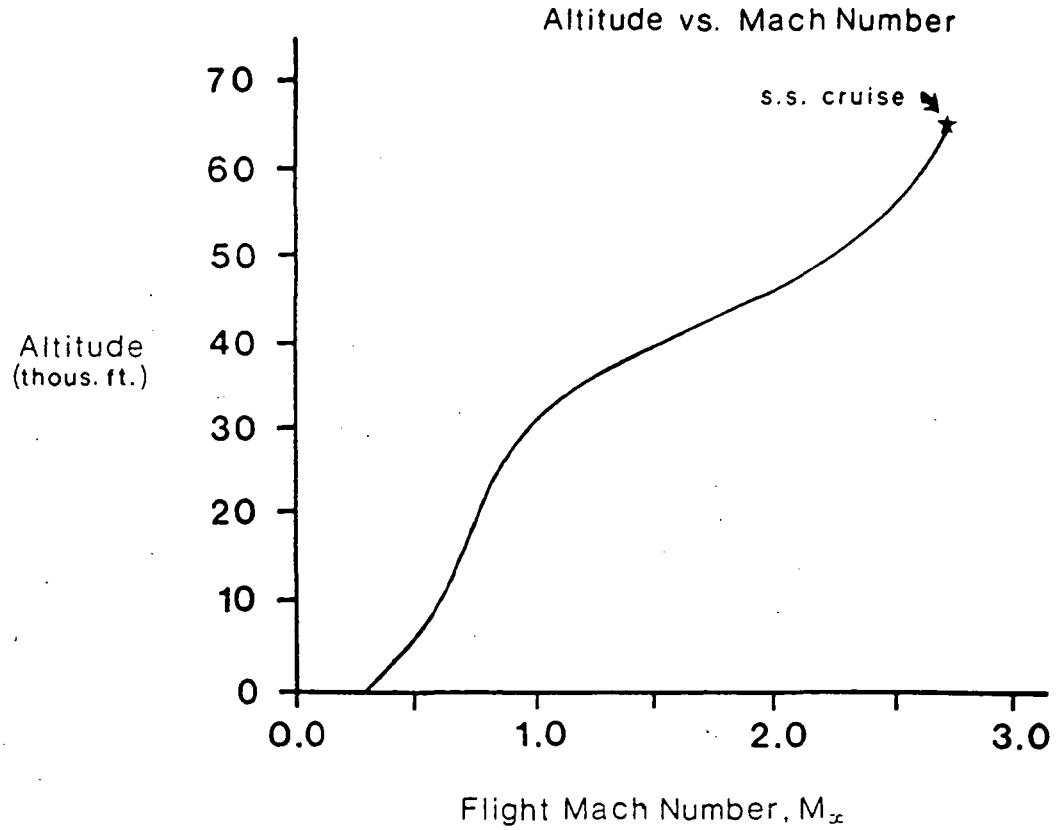

Figure 2.1 Mach Number-Altitude Profile of Baseline Mach 2.7 SST Mission

Flight Mach No.	Altitude (ft)	Pressure (lb/ft^2)	Temp (°R)	Speed of Sound (ft/sec)
0.00-0.30	0	2116.2	518.4	1116.2
0.60	10,000	1455.1	479.2	1077.1
0.95	30,000	627.9	411.4	994.3
1.60	40,000	334.8	392.4	971.2
2.20	50,000	243.2	392.4	971.2
2.70	65,000	118.7	392.4	971.2

Table 1. Characteristics of the Standard Atmosphere at Selected Altitudes in the Mission Profile

2.1.2 AIRFRAME THRUST REQUIREMENTS

The Baseline Aircraft is a 650,000 lb. TOGW SST fitted with four engines. Briefly the Airplane's Thrust requirements are as follows:

1. Minimum ratio of Thrust/T.O.G.W. 0.28 at Mach 0.30
2. Thrust Margin during Accereration: Thrust/Drag >1.2 at all points during climb and acceleration.

The numerical values of these constraints for the baseline aircraft as interpreted from Reference 1 are presented in Figure 2.2. These outline the thrust required per engine.

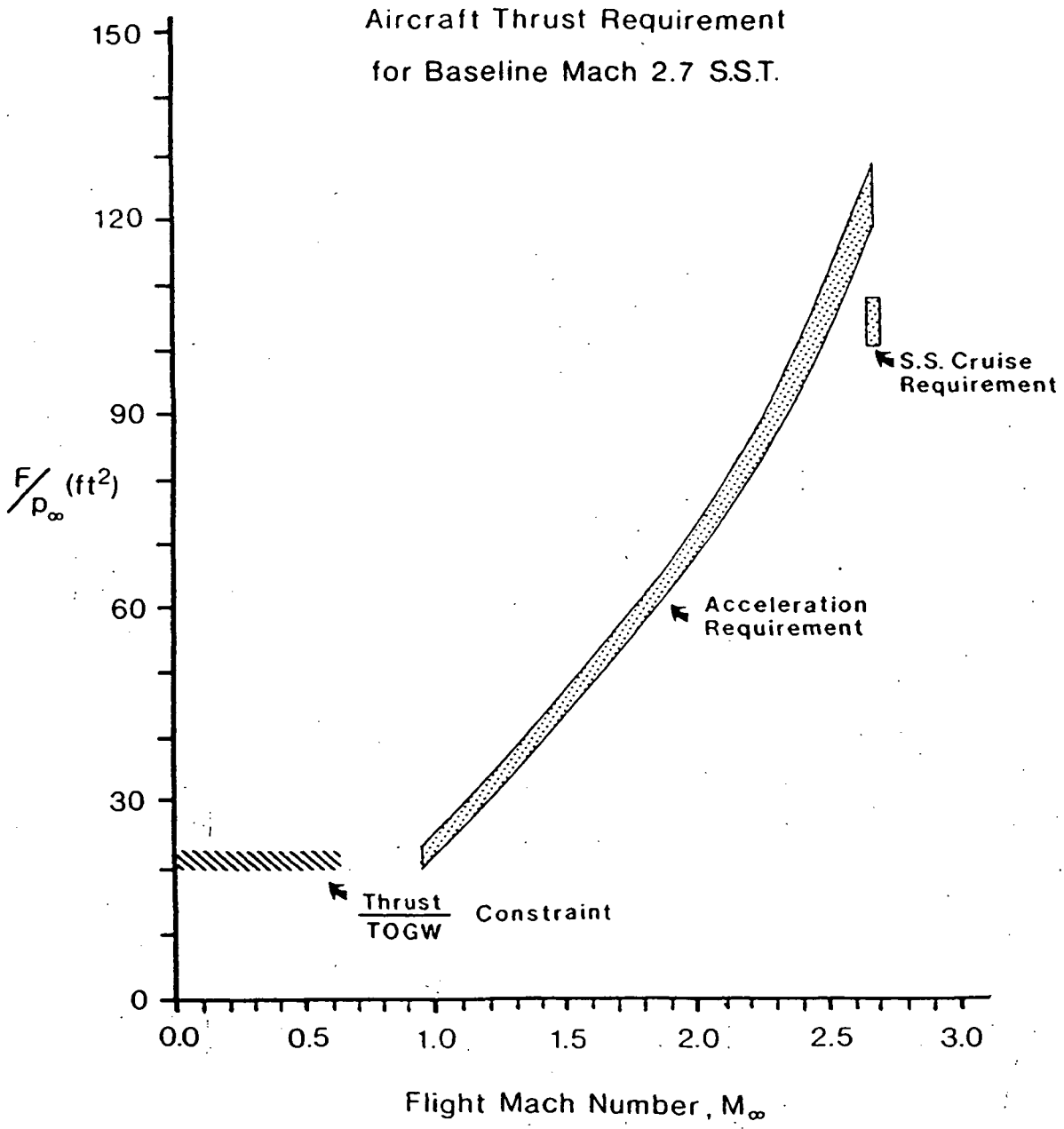

Figure 2.2 Thrust Requirement for Baseline Mach 2.7 SST

2.2 CYCLE ANALYSIS

The quantitative or non-ideal cycle analysis was carried out according to standard methods outlined in References 3 and 4. A FORTRAN program was developed to carry out the numerical computation. A summary of the methods used and a listing of the computer program are presented in Appendix A.

All cycle calculations represent uninstalled performance values. No attempt was made to estimate or compare losses due to cowl and nacelle drag or interference effects between engine and airframe.

2.2.1 EFFECT OF DIFFUSER PRESSURE RATIO ON SPECIFIC IMPULSE AT DESIGN POINT

It is very important to extract maximum efficiency from the fan diffuser if a bypass engine is to be used. For engines which operate at Mach numbers substantially greater than 1, diffuser total pressure losses due to shocks can be quite significant. For example, at Mach 2.7, a normal shock produces a pressure recovery of 0.42. Since the total pressure rise across a fan stage is significantly lower than that across a fan stage is significantly lower than that across the core compressor, it is to be expected that performance of a bypass engine can be severly impaired by poor diffuser performance.

A study was therefore performed to assess the effects of diffuser performance on the specific impulse of a bypass engine which uses the same diffuser for both core and bypass flow. (i.e. this might represent a turbofan with conventional axially subsonic fan.)

This was carried out for bypass ratios of 0, 1, and 2. The gas generator efficiencies and pressure ratios was the same for all bypass ratios, as were fan stage component effieiencies. The flight condition modeled was cruise at Mach 2.7.

Particulars are as follows:

Engine Parameters: $\pi_c = 14.6$ $\pi_c' = 2.8$ $T_{t4} = 3200°R$

$\pi_b = 0.98$ $\eta_b = 0.99$ $\pi_n = \pi_n' = 0.98$

$e_c = 0.85$ $e_c' = 0.85$ $e_t = 0.90$

The diffuser pressure recovery factors were allowed to range from 0.65 to 1.00. The results are plotted in Figure 2.3. The principal result for this is that if diffuser efficiency is poor, the performance of the engine in terms of specific impulse can fall below that of a dry turbojet.

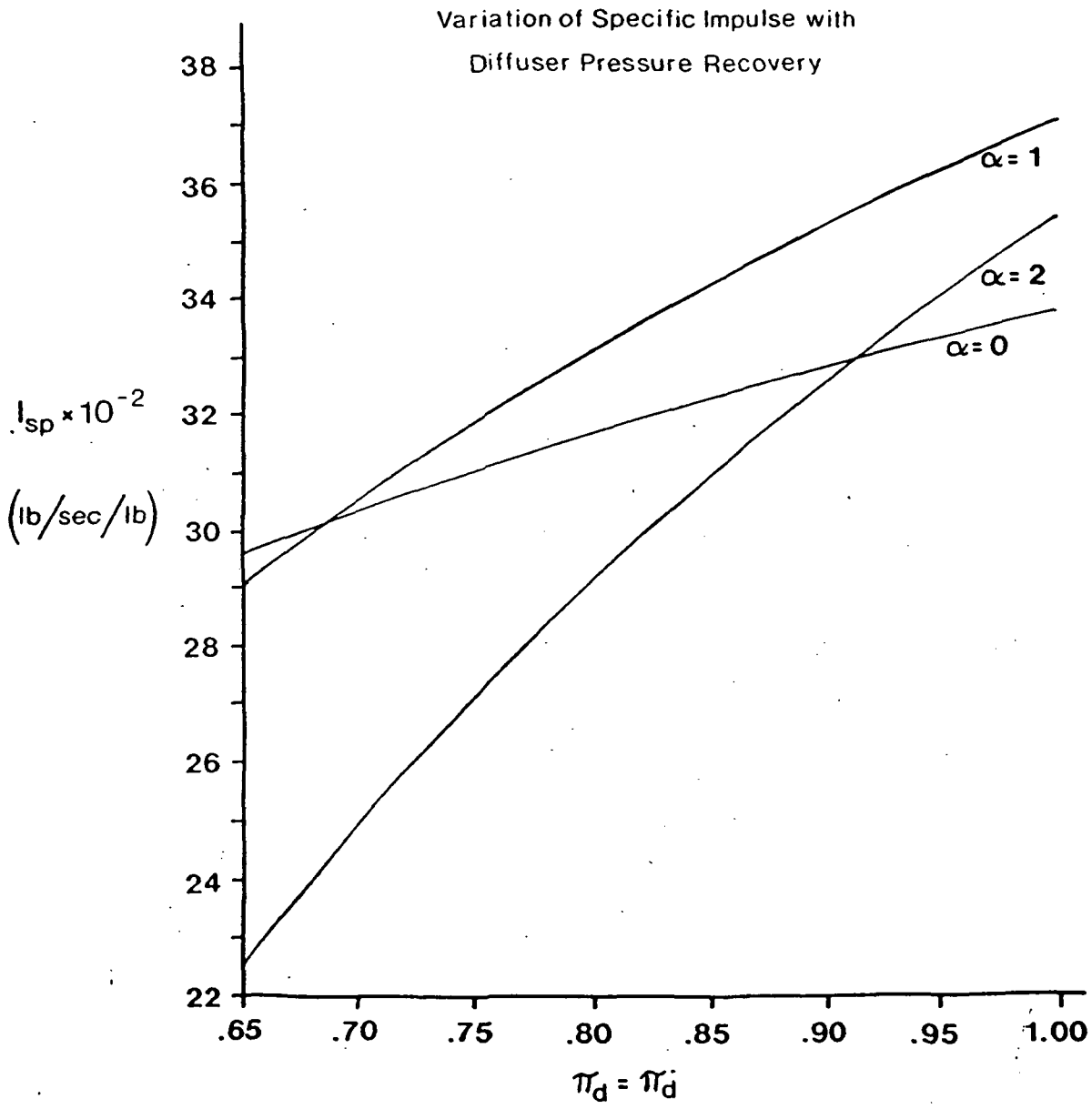

Figure 2.3 Variation of Specific Impulse with Diffuser Pressure Ratio for Conventional Bypass Engine

2.2.2 IMPROVEMENT IN SPECIFIC IMPULSE OFFERED BY INCREASE IN DIFFUSER PRESSURE RECOVERY IN SUPERSONIC FAN FOR VARIOUS CORE PRESSURE RECOVERIES.

As shown in the previous section, the total pressure ratio in the diffuser can have a significant effect on engine performance. If instead of a conventional subsonic turbofan, the engine is fitted with a fan which can accept supersonic axial Mach numbers, less diffusion is required for the bypass flow. Presumably, this would reduce diffuser losses and lead to an improvement in specific impulse.

For this analysis, it is assumed that only a small amount of diffusion will take place in front of the fan and that the pressure recovery factor is 0.97. This figure is consistent with the inlet geometry discussed in Section 2.3.

It is found that the optimum bypass ratio for the S.S. fan engine is around 1.16. Hence, this was the bypass ratio used in comparing the superflow engine to the conventional turbofan. For the comparison, all engine parameters except the fan diffuser pressure ratio are the same for both engines. The core flow pressure ratio is allowed to vary from 0.65 to 1.00. The specific impulse of these engines at the Mach 2.7 cruise condition is plotted as a function of core pressure recovery in Figure 2.4. The principal trend observed is that the supersonic fan equipped engine shows diminishing advantage over the conventional turbofan as the pressure recovery of the supersonic-subsonic diffuser is increased. However, even with

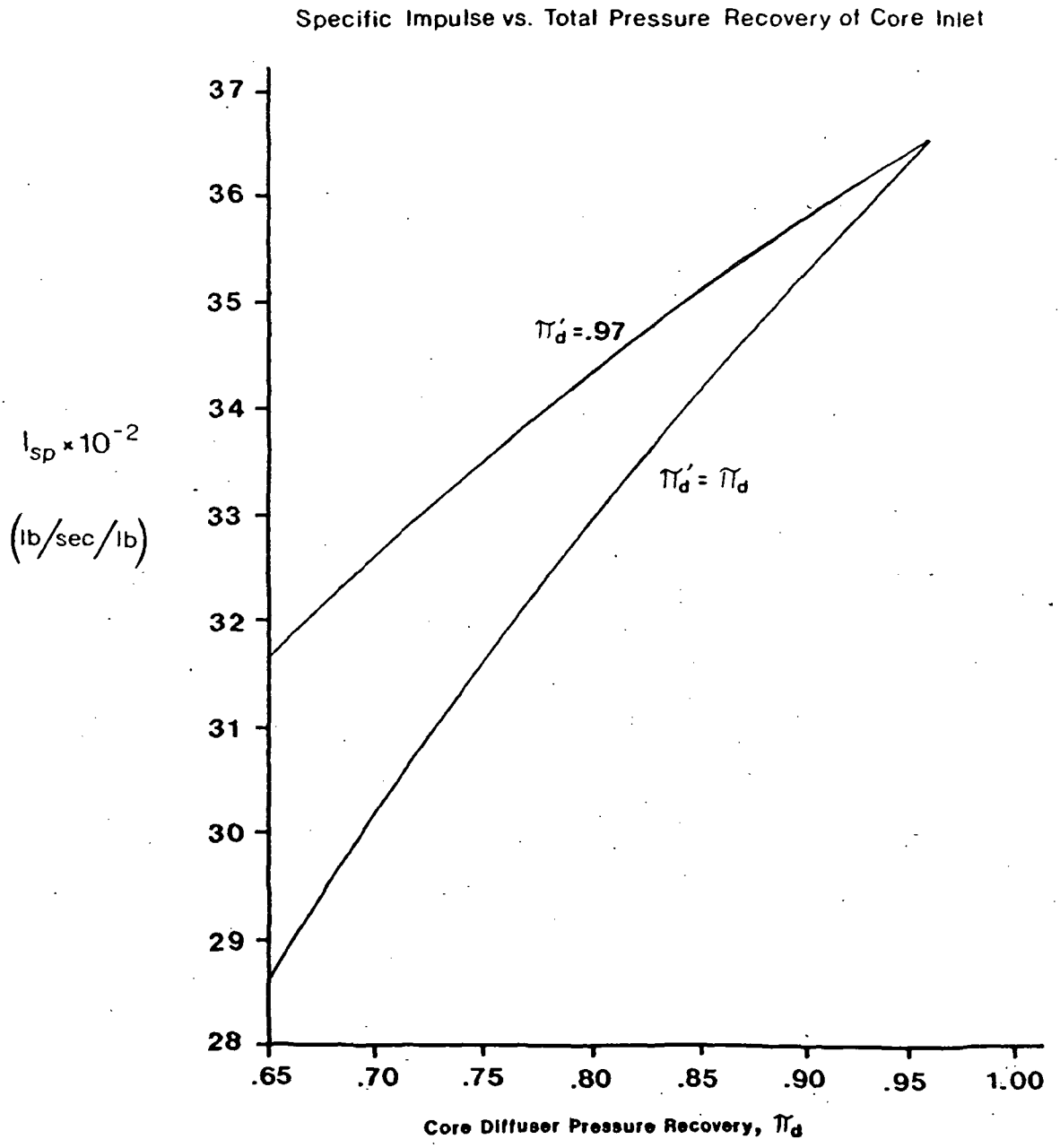

Figure 2.4 Variation of Specific Impulse of Supersonic Fan Engine and Conventional Turbofan with Diffuser Pressure Ratio

the core diffuser pressure recovery at .87, the superflow engine has a 2% higher specific impulse due to better pressure recovery in the fan inlet.

2.2.3 SIZING ENGINES FOR 650,000 lb. TOGW SST AND COMPARISON WITH CONVENTIONAL POWER PLANTS

In sizing the engine, the two chief constraints considered were providing sufficient airflow at the Mach 2.7 supersonic cruise design point to provide sufficient thrust at the operating point giving best SFC, and capturing enough mass flow in the takeoff configuration to meet the thrust to weight ratio of 0.28.

For the superflow engine with the specified fan pressure ratio, core compressor pressure ratio, bypass ratio, and turbine inlet temperature, the overriding constraint is the thrust to weight ratio at Mach 0.30. The superflow engine sized to meet this has a total weight flow of 1520 lbs./sec. at sea level static conditions. The static thrust per engine is 58,400 lbs. This engine exceeds by a fair margin the required thrust during supersonic acceleration and at Mach 2.7 cruise closely matches the thrust requirement. By comparison, a conventional turbofan with the same bypass and pressure ratios would require 702 lb/sec at Mach 2.7 as compared to 687 lb/sec for the superflow engine. These figures represent total airflow. A second comparison may be made with a conventional turbojet with compressor pressure ratio optimized for best S.F.C. at Mach 2.7 cruise. With a compressor pressure ratio of 24.0, the turbojet would have a significantly larger gas generator than the fan engines with an airflow of about 670 lb/sec.

Figure 2.5 shows a rough size comparison between the superflow engine and a turbojet producing the same thrust with an airflow of 1000 lb/sec. at takeoff. This sketch is based on

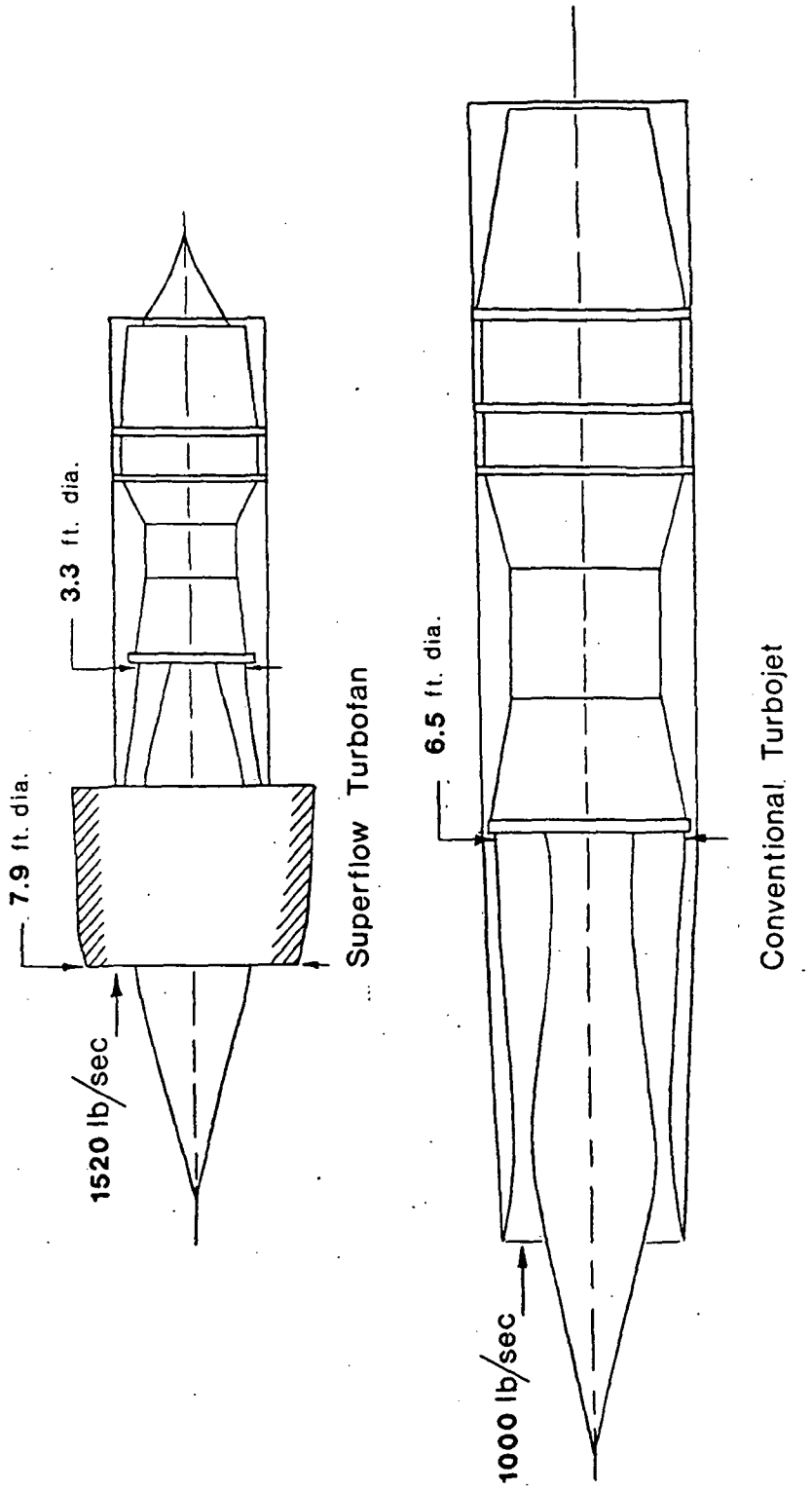

_Figure 2.5 Approximate Size Comparison Between Superflow Turbofan and a Conventional Turbojet

dimensional data from Reference 1.

2.2.4 OPTIMIZING BYPASS RATIO FOR BEST SPECIFIC IMPULSE AT MACH 2.7 CRUISE

For a gas generator with given characteristics of component efficiencies, compressor pressure ratio, turbine inlet temperature and a fan of given efficiency and pressure ratio, the bypass ratio can be varied to find the optimum bypass ratio at any flight condition. This was carried out at the Mach 2.7 cruise condition for an engine with the following characteristics:

Core: $\pi_d = 0.87$ $\pi_c = 14.6$ $T_{t4} = 3200°R$ $\pi_b = 0.98$ $\eta_b = 0.99$
$e_c = 0.85$ $e_t = 0.90$ $\pi_n = 0.98$

Fan: $\pi_d' = 0.97$ $\pi_c' = 2.8$ $e_c' = 0.85$ $\pi_n' = 0.98$

The specific impulse is plotted as a function of bypass ratio in Figure 2.6. The specific thrust and specific impulse are maximized at a bypass ratio of 1.16. The specific thrust is 1.287 per unit of core airflow and 0.592 per unit of total airflow. The value of the specific impulse is 3540 (lb/sec/lb). (SFC=1.02 lb/hr/lb).

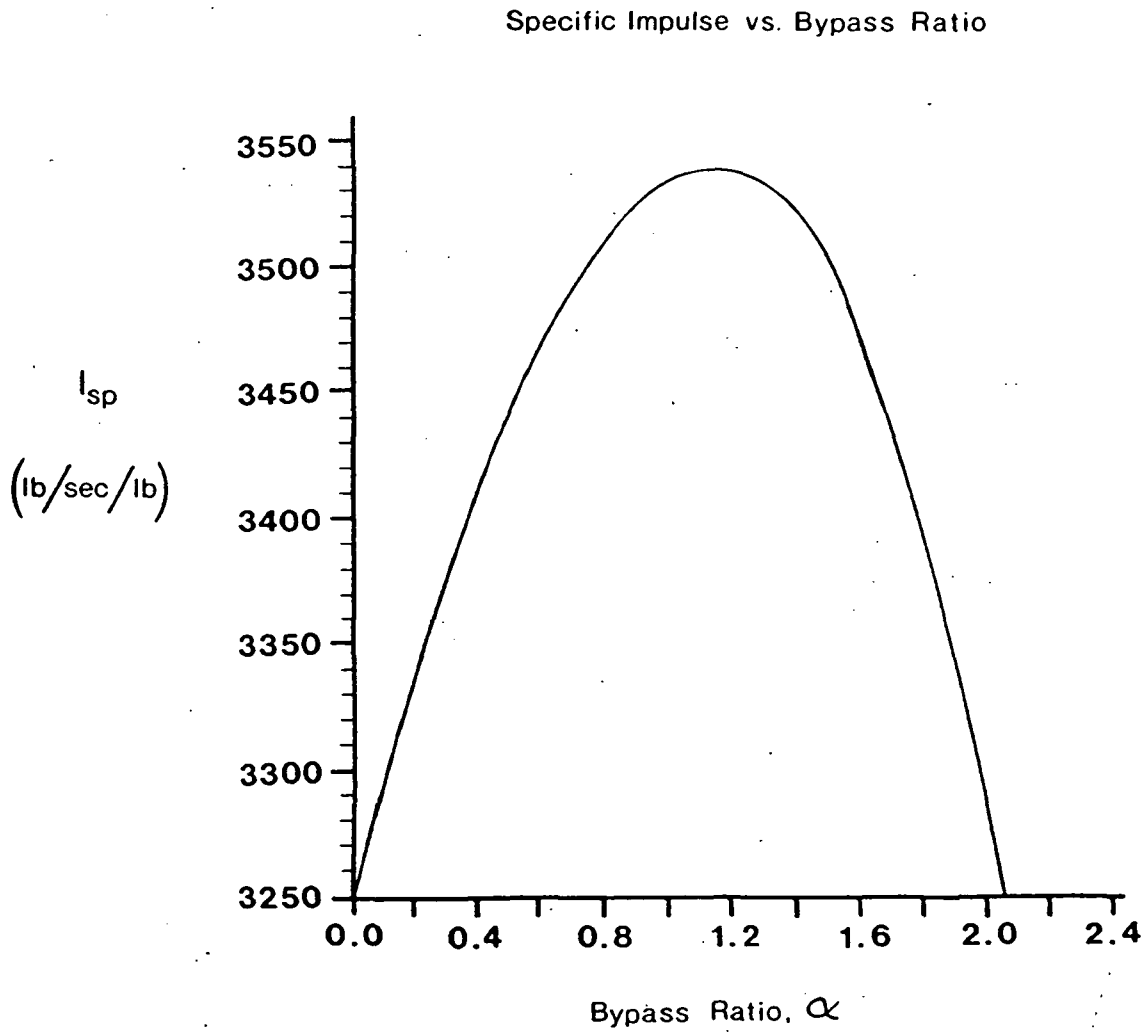

Figure 2.6 Effect of Bypass Ratio on Specific Impulse of Supersonic Fan Engine

2.2.5 EFFECT OF FAN EFFICIENCY ON SPECIFIC IMPULSE AT MACH 2.7 CRUISE

The effect of fan efficiency on specific impulse of the superflow engine at Mach 2.7 was carried out by variation of the polytropic exponent for the fan stage. As a comparison, the variation in performance is compared in Figure 2.7 with the performance of a turbojet using the same gas generator. The component efficiencies for these engines are as follows:

Turbojet: $\pi_d = 0.87$ $\pi_c = 14.6$ $T_{t4} = 3200°R$ $\pi_b = 0.98$ $\eta_b = 0.99$
$e_c = 0.85$ $e_t = 0.90$ $\pi_n = 0.98$

Supersonic Fan:
$\pi_d = 0.87$ $\pi_c = 14.6$ $T_{t4} = 3200°R$ $\pi_b = 0.98$ $\eta_b = 0.99$
$e_c = 0.85$ $e_t = 0.90$ $\pi_n = 0.98$
$\pi_d' = 0.97$ $\pi_c' = 2.8$ $\alpha = 1.16$ $\pi_n' = 0.98$

The principal result of this calculation is that if the fan polytropic efficiency falls below .68 or so, the advantage of a bypass fan is outweighed by the reduced efficiency of the rotor.

It is worthwhile to point out that in mechanical arrangements where the rotor makes up the first stage of the core compressor, loss of efficiency in the fan rotor will be reflected in a loss of efficiency in the core compressor as well.

2.2.6 EFFECT OF CORE COMPRESSOR EFFICIENCY ON SPECIFIC IMPULSE AT MACH 2.7

The effect of core compressor efficiency on the specific impulse of the superflow engine at Mach 2.7 cruise was carried out by variation of the polytropic exponent for the compressor. The effect of this value on specific impulse at the design point is plotted in Figure 2.8. The component efficiencies of the engine are as follows:

$$\pi_d = 0.87 \quad \pi_d' = 0.97$$

$$\pi_c = 14.6 \quad \pi_c' = 2.8 \quad T_{t4} = 3200^\circ R$$

$$\pi_b = 0.98 \quad \eta_b = 0.99 \quad \pi_n = \pi_n' = 0.98$$

$$\alpha = 1.16 \quad e_c' = 0.85 \quad e_t = 0.90$$

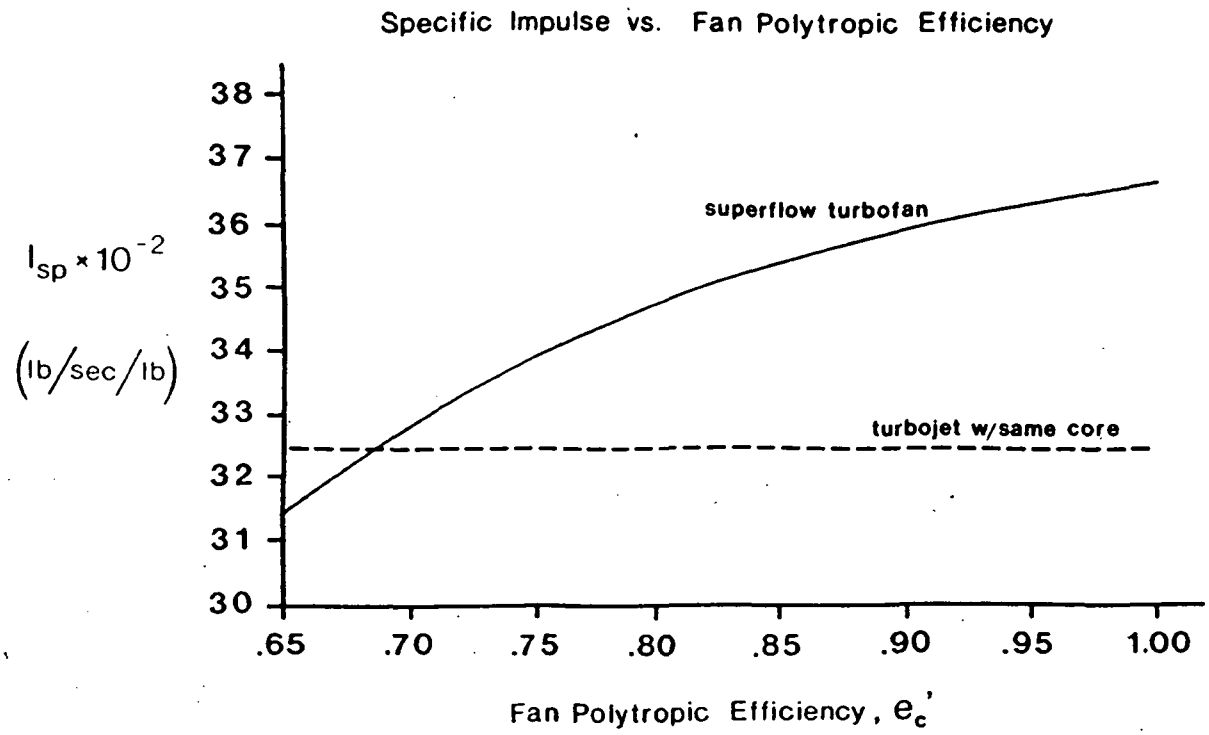

Figure 2.7 Effect of Fan Polytropic Efficiency on Specific Impulse at Mach 2.7 Cruise

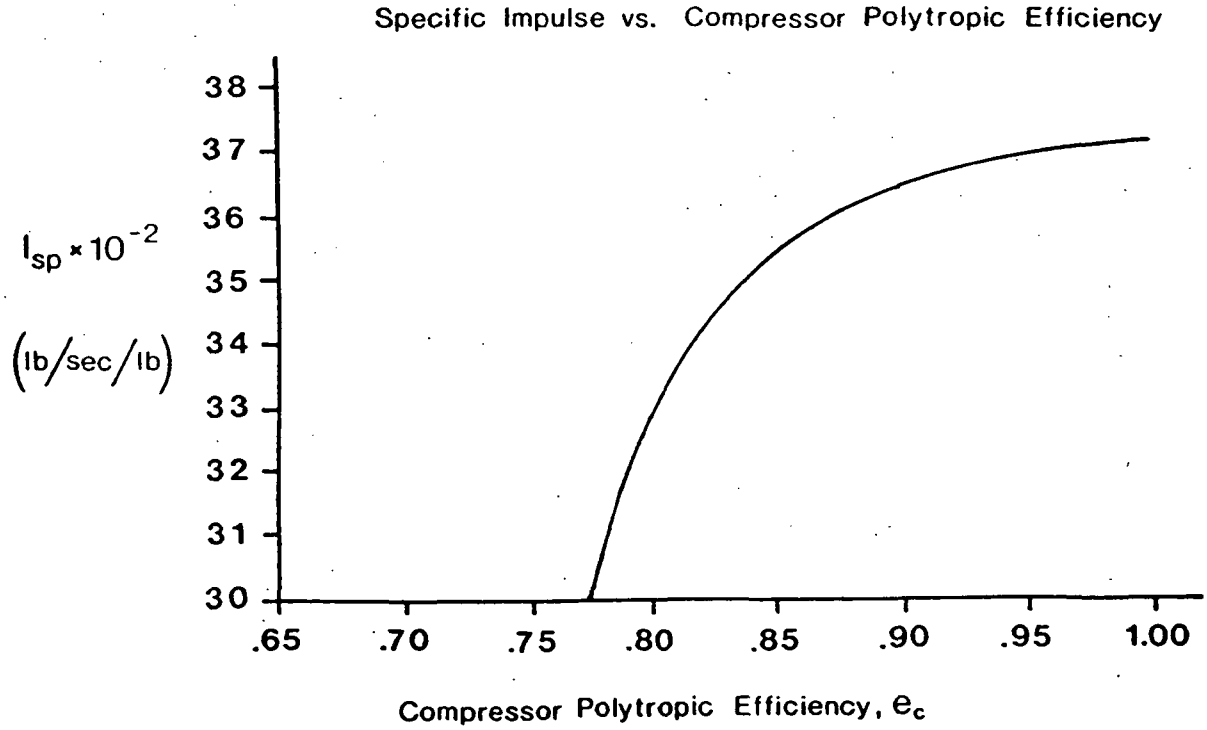

Figure 2.8 Effect of Core Compressor Polytropic Efficiency on Specific Impulse at Mach 2.7 Cruise

2.2.7 MATCHING OF SUPERFLOW ENGINE TO THRUST REQUIREMENTS THROUGHOUT FLIGHT ENVELOPE

A quantitative cycle analysis of the superflow engine was performed over the range of mission flight Mach numbers and the results compared with the airframe thrust requirement. The component efficiencies and characteristics used for the analysis are as follows:

$$\pi_d = 0.87 \quad \pi_d' = 0.97$$
$$\pi_b = 0.98 \quad \eta_b = 0.99 \quad \pi_n = \pi_n' = 0.98$$
$$e_c = 0.85 \quad e_c' = 0.85 \quad e_t = 0.90$$

The fan and compressor pressure ratios, bypass ratio, and turbine inlet temperature follow the schedule outlined in Reference 1. These quantities are tabulated in Table 2. The mass flow schedule corresponds to choked conditions in front of the fan for subsonic Mach numbers and that dictated from inlet conditions for supersonic Mach numbers. The inlet used is described in Section 2.3. The specific thrust of the engine compared to the thrust requirement is plotted in Figure 2.9.

	M_∞	π_c	π_c'	α	T_{t4} (°R)
	0.00	24.0	3.0	1.80	2550
	0.30	24.0	3.0	1.81	2550
	0.60	31.8	3.7	1.56	3250
Acceleration	0.95	32.7	3.8	1.50	3060
	1.60	30.5	3.5	1.55	3400
	2.20	21.7	3.1	1.36	3400
	2.70	14.6	2.8	1.16	3400
S. S. Cruise ➡	2.70	14.6	2.8	1.16	3200

Table 2. Schedule of fan and compressor ratios, bypass ratio, and turbine inlet temperature for Superflow Engine during acceleration and supersonic cruise.

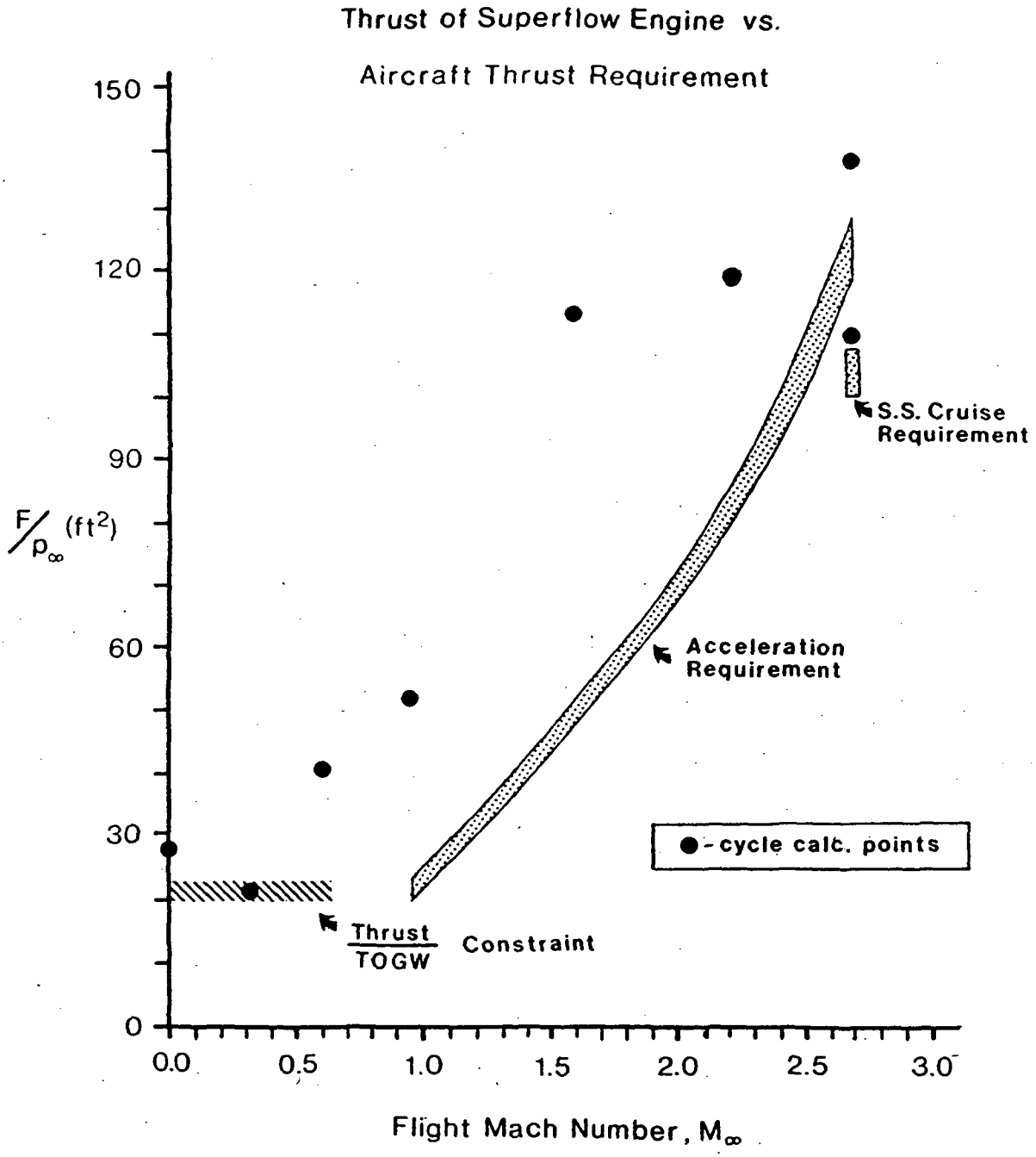

Figure 2.9 Thrust of Superflow Engine Compared to Thrust Requirement for Baseline Mach 2.7 SST

2.3 INLET DESIGN

In the overall assessment of the supersonic through flow engine, the technical feasibility of an inlet with the specified mass flow schedule and pressure recovery is an important consideration. As shown in the cycle analysis, the performance advantage offered by the bypass engine is quite sensitive to the pressure recovery of the fan inlet.

Secondly, for an aircraft flying at supersonic speeds with the inlet started, the fan can exert no upstream influence and hence the mass flow to the engine is dictated by the fan inlet. For the supersonic fan engine at subsonic speeds, it has been proposed to operate with the flow choked at the fan face. This dictates an inlet with the minimum flow area at the fan face, at least while flying subsonically.

It has been found that a fixed geometry inlet with straight conical spike provides the required mass flow schedule throughout the flight envelope with an acceptable level of pressure recovery. For the purpose of the design study, the calculated performance of this type of inlet sets a baseline for diffuser performance from a standpoint of shock losses and capture that can be expected. Potential advantages and problem areas of more sophisticated inlet designs can be compared with it.

However, the simple conical spike has advantages of its own. First, is its simplicity. This probably leads to light weight without variable geometry mechanisms, and a shape which is easy

to make structurally robust. Secondly, at zero degrees angle of attack, the cone boundary layer is not subjected to a pressure gradient, except perhaps for a small pressure rise inside the fan cowl. So called isentropic compression inlets which achieve pressure rise by a nearly continuous pressure rise on the surface of the spike can in principle reduce shock losses, but these are prone to separation problems. Angle of attack changes can lead to inlet distortion problems and an increase of the pressure gradient. Conversely conical spike inlets can be made quite insensitive to angle of attack.

Choked flow at the fan face at subsonic operation conditions sets the flow area required at the fan face. At the supersonic design point, the inlet is configured so that the conical shock originating at the tip of the spike intersects the cowl lip in the interest of minimizing wave drag at this flight condition. Additionally, it is desired to make the cone angle as large as possible to make the spike as short as possible for weight and structural reasons. However, there are limits to the cone angle which can be used for the following reasons:

a)Shock loss from the conical bow shock increases with cone angle.

b)Requirement to keep shock attached to cone down to relatively low Mach number.

c)Necessity to fair the cone to the rotor with the desired

hub to tip radius ratio. It is desired to make the cone surface Mach number marginally above that which will prevail at the fan face.

d)Necessity to limit "supersonic spill" in off design flight conditions to meet mass flow constraint.

For purposes of the design study, it has been assumed that the inlet meets the air at the flight Mach number of 2.7. (This may be modified by engine mounting locations in which the inlets are placed aerodynamically in the proximity of the wing or other components.) A cone half angle of 16 degrees and an annulus area of 30.7 ft^2 meets the outlined constraints for an engine with a sea level static mass flow of 1520 lb/sec. A dimensioned sketch of the inlet is shown in Figure 2.10 and Figure 2.11 illustrates the capture schedule of this inlet compared to that required to meet minimum mass flow requirments. At the design point, the pressure ratio of the conical shock is 0.99 leaving a 2 % margin to meet the target pressure recovery of 0.97. The shock angle variation at off design conditions are shown in Figure 2.12.

A little explanation of Figure 2.11 is in order. The discrepancy between the required capture schedule and that provided by the 16 degree conical spike inlet should not be interpreted as a gross mismatch of inlet to engine. The triangle points represent the minimum airflow required to meet thrust constraints when the engine is operated with cycle parameters from Table 2. Hence, the increase in airflow provided by the

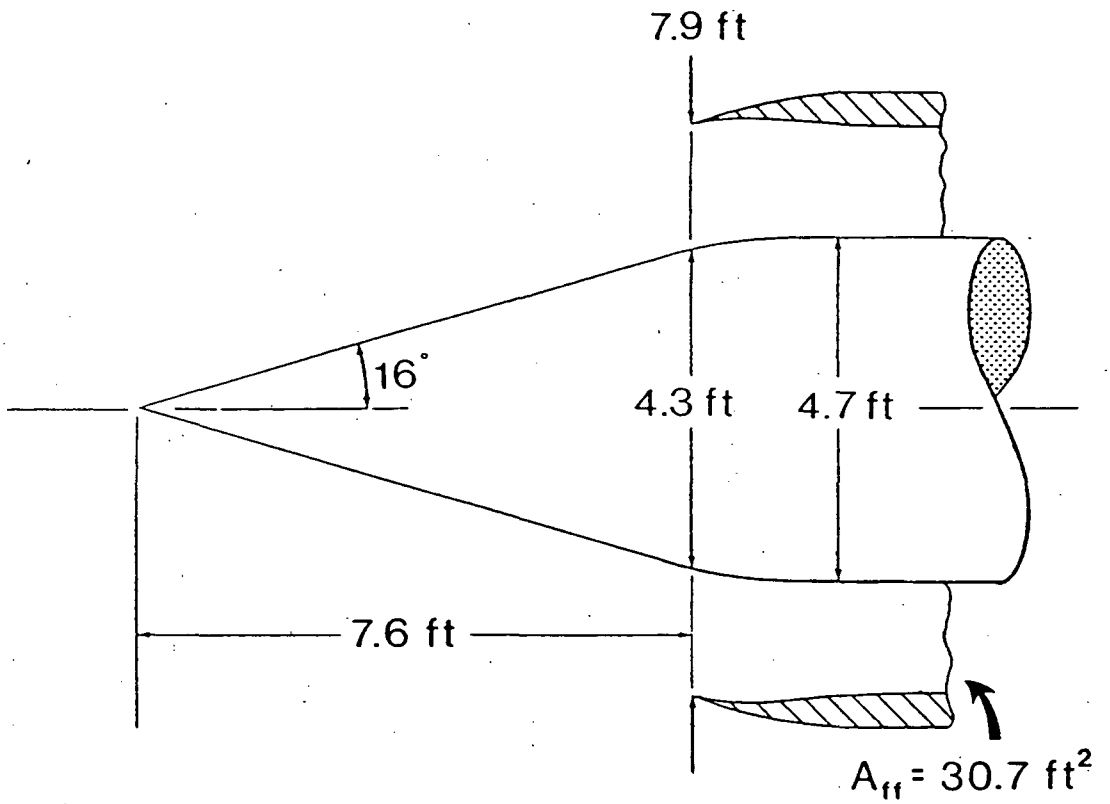

Figure 2.10 Dimensions of 16° Conical Spike Inlet

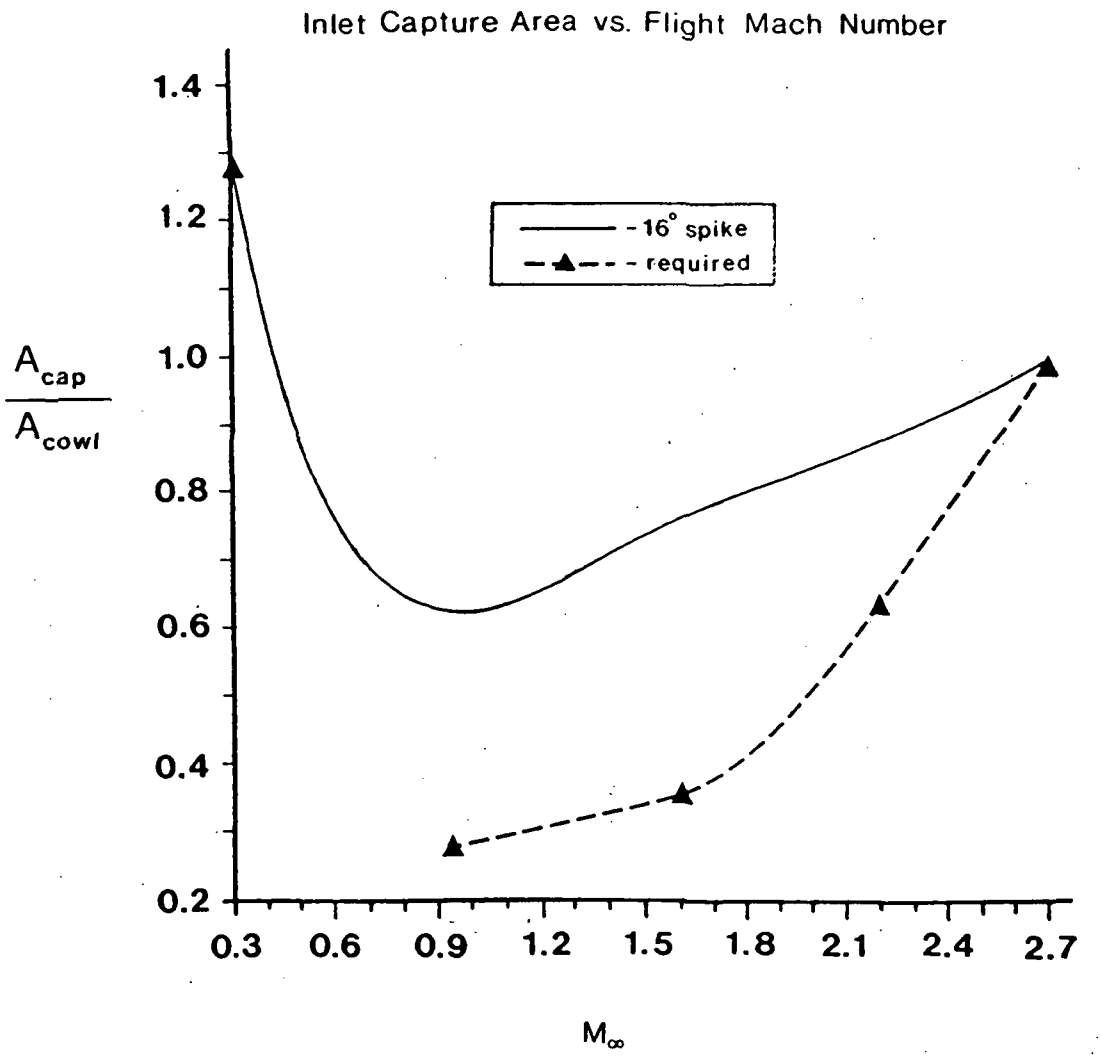

Figure 2.11 Capture Schedule of 16° Conical Spike Inlet Compared to Capture Schedule Required to Meet Thrust Constraint

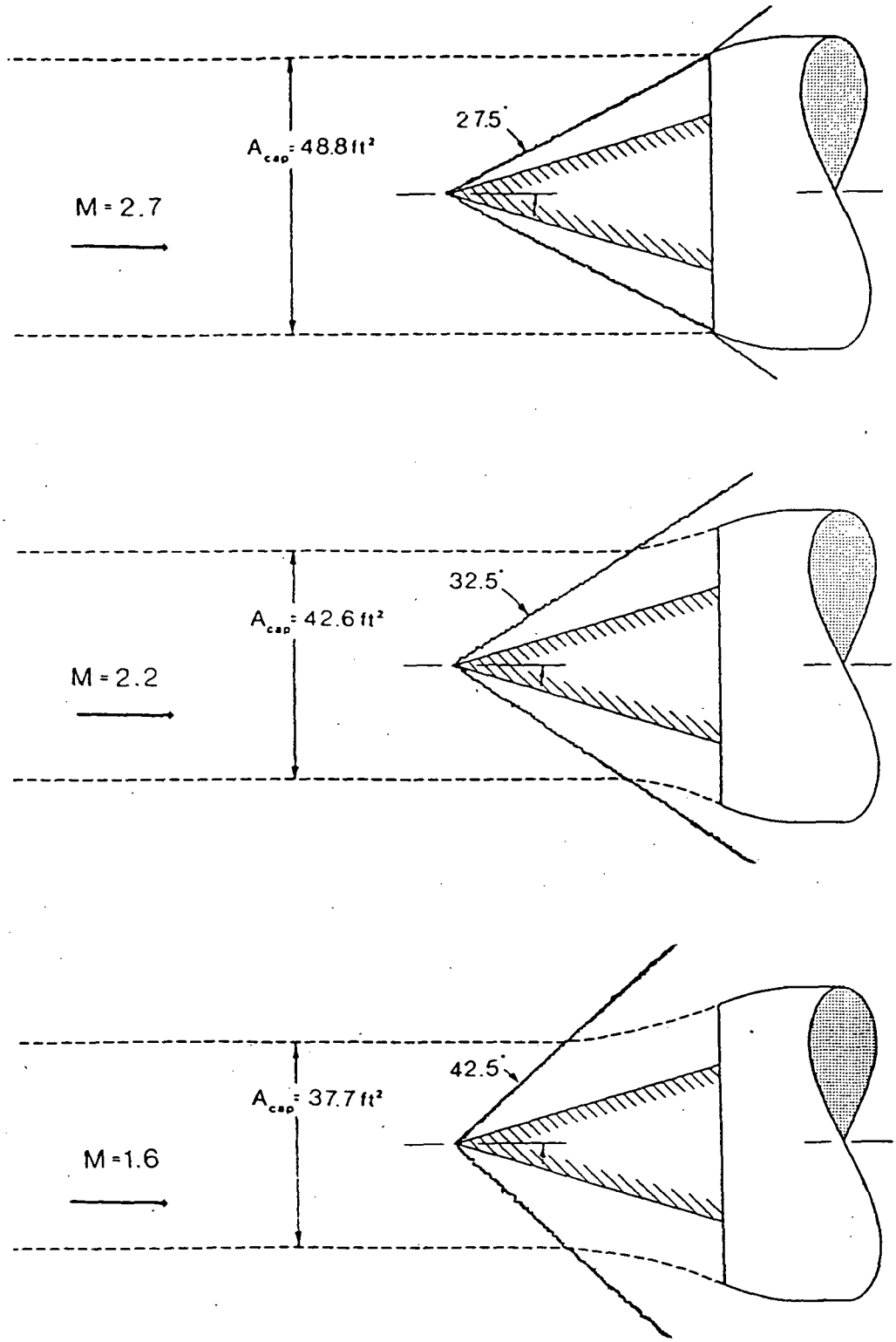

Figure 2.12 Variation of Spike Shock Angle with Flight Mach Number

inlet during much of the acceleration, produces a surplus of thrust. However, in looking at an engine geometry in detail, it must be verified that the gas generator can process the captured airflow.

2.4 SUMMARY OF SYSTEM STUDY

The system study performed herein serves to show the relative merits of employing a bypass fan in an engine designed to operate at high Mach number. The diffuser pressure recoveries tend to figure significantly in the balance of whether the bypass engine offers an improvement in uninstalled specific impulse over the turbojet or more conventional bypass engines. At high Mach numbers, the pressure recoveries of supersonic-subsonic diffusers tend to deteriorate and the development of a fan which could accept axially supersonic flow is a unique solution to this problem.

However, this is only part of the story. As pointed out in Chapter 1, part of the advantage of the superflow engine lies in lower installation losses, due to smaller, less complex, fan cowls and nacelles. These factors were not taken into account in this investigation, and all cycle analysis results represent uninstalled performance figures. If the concept is pursued further and a detailed geometry defined, the installation losses must be seriously considered, both from the standpoint of cowl and nacelle drag, and that of interference between engine and airframe. Otherwise, the performance improvement offered by the superflow engine concept may not be realized.

3. BLADING DESIGN FOR SUPERSONIC THROUGHFLOW FAN

SYMBOLS

The following symbols are used in this chapter:

A	flow area
c	chord length
D_{loc}	local diffusion factor (based on local velocities)
i	incidence angle, angle between intet-air direction and tangent to blade mean camberline at leading edge in degrees
M	Mach number
p_t	total or stagnation pressure
p	static pressure
s	blade spacing
v	air velocity
z	coordinate along axis
β	air angle, angle between velocity vector and axial direction in degrees
δ	leading edge half angle
K	blade angle, angle between tangent to blade mean camber line and axial direction in degrees
φ	blade camber angle, difference between blade angles at blade leading and trailing edges, $K_1 - K_2$ degrees
$\tilde{w}$	total-pressure loss coefficient
θ	flow deflection angle (in reference to shock waves forming)
Γ	shock wave angle relative to incident flow
σ	solidity
ν	Prandtl-Meyer angle
η_{stage}	Stage adiabatic efficiency

The nomenclature and symbols for designating velocity triangles as used in this report for a fan stage made up of a rotor and stator are represented in Figure 3.1. The notation and symbols describing cascade geometry and flow angles are shown in Figure 3.2.

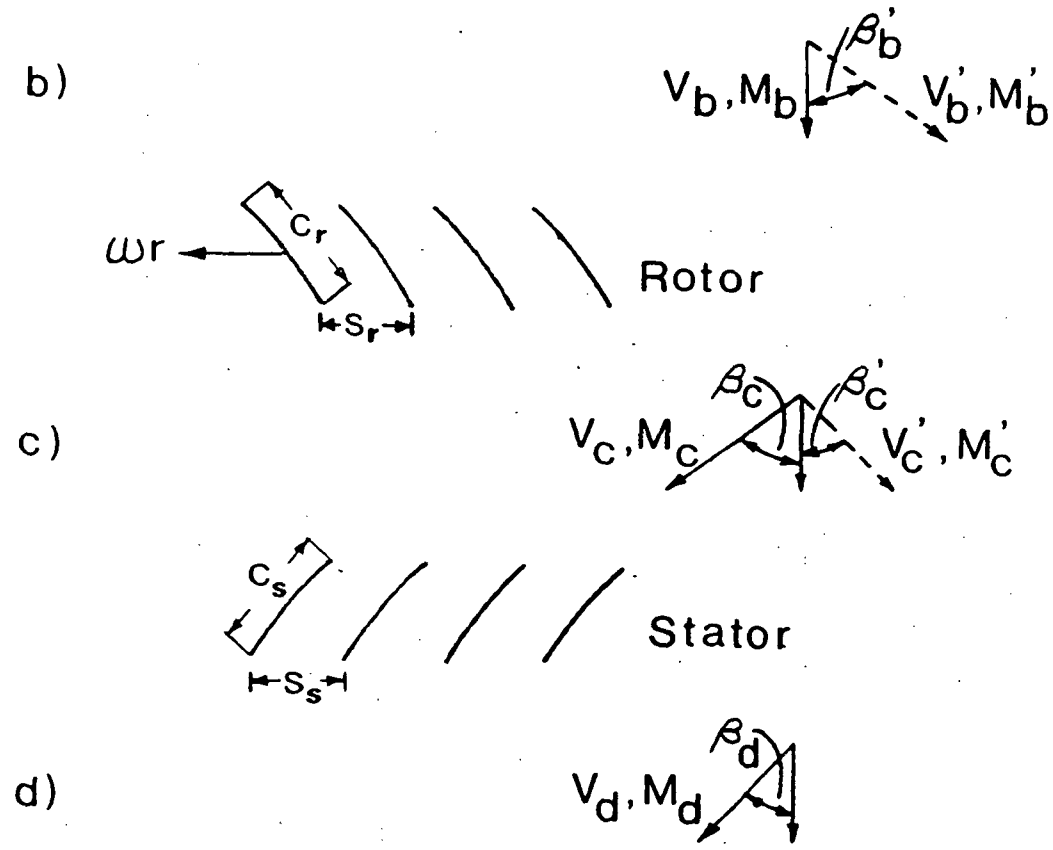

Figure 3.1 Development of velocity diagram for a rotor-stator fan stage.

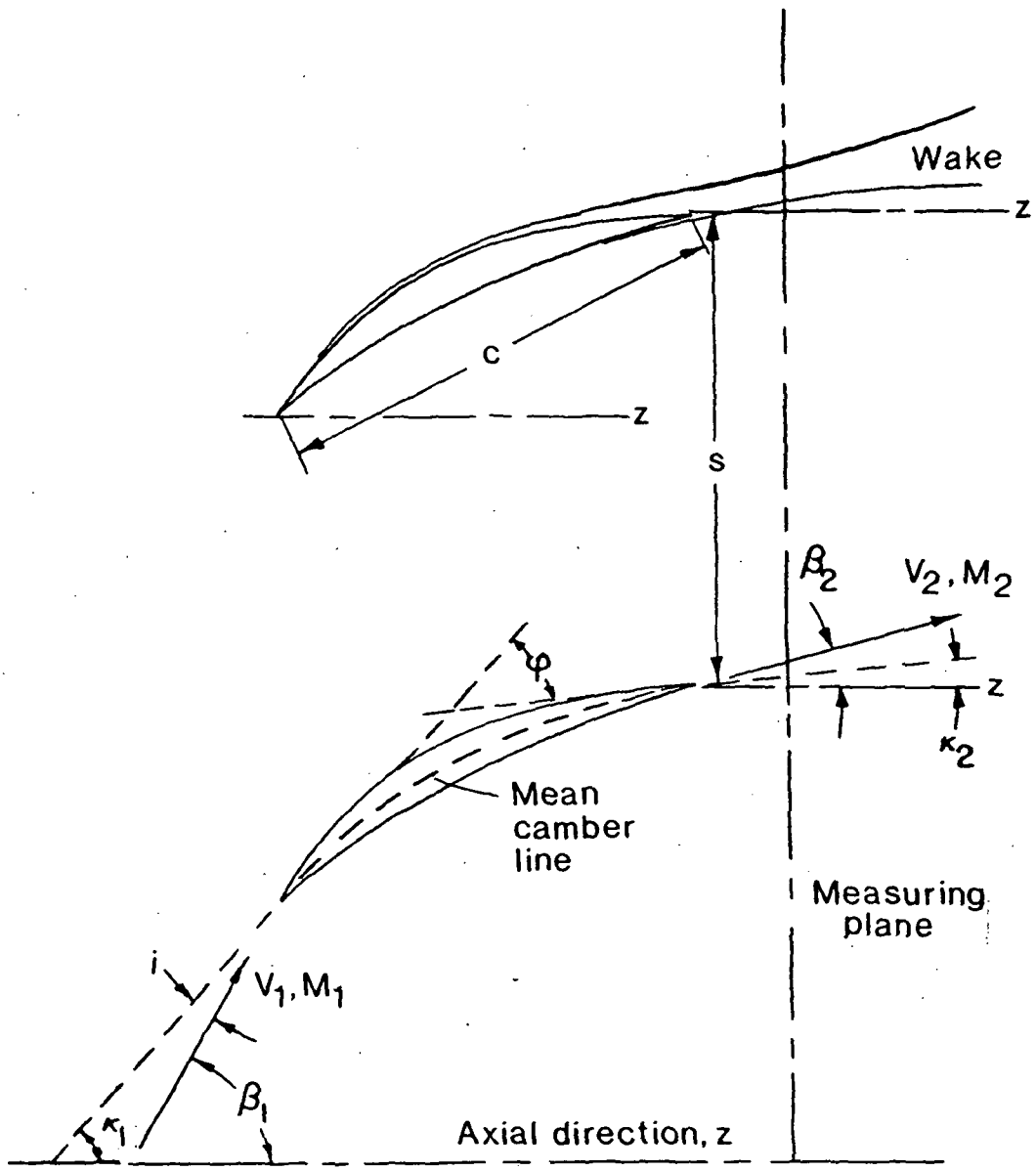

Figure 3.2 Cascade notation.

3.1 BACKGROUND

Very little in the way of analytical predictions or experimental data exists on turbomachinery with supersonic axial velocity, with work on blading applicable to a supersonic fan being almost non-existent.

Some work has been performed since the 1950's in the area of supersonic compressors. Most of this pertained to machines with subsonic axial velocities, but supersonic relative velocities, and these can be separated into two types, namely shock in rotor and shock in stator compressors. The shock in rotor variety, as the name implies, produces transition from supersonic to subsonic relative velocities in the rotor by means of shocks within the rotor passage. This transition is accompanied by a substantial static pressure rise and the flow enters the stator with subsonic velocity. The shock in stator compressor turns the flow in the rotor while maintaining supersonic relative velocity and the diffusion to subsonic velocity occurs in the stator. Very few experimental results exist for this type, most experimental work having been performed on stages of the former type. (See Refs. 6 & 7.)

The results of these experiments were for the most part disappointing with measured stage efficiencies being lower than predicted. However, tests performed by Daimler-Benz (1968) on impulse type rotors with downstream stator removed have shown adiabatic efficiencies as high as 95%. See Reference 1.

More recently, Breugelmans (1975) published results of experiments on an isolated rotor designed to accept flow with an axially supersonic flow at the face of the rotor. This rotor employed blades with 25 degrees of camber at the mid-blade radial station and had a hub to tip ratio of 0.75. At 100% design rotor speed the axial Mach number was intended to be 1.5 with a tip tangential Mach number of 2.0 based on inlet total conditions.

This rotor was never tested beyond 90% of design speed due to mechanical failure. However, at this operating point the axial Mach number was 1.5 and the relative Mach number at the tip was 2.4. This is the sole example of experiments performed on an axially supersonic rotor known to this author. (See Refs. 11 & 12.)

Breugelmans' rotor design was not pursued for this study as its axial Mach number was too low and its rotational speed too high for the fan rotor of the superflow engine. It was proposed for this investigation to perform only minimal diffusion of the free stream flow, from Mach 2.7 to Mach 2.2 at the fan face. Secondly, the design tangential Mach number of the Breugelmans rotor translates to a physical speed of about 3000 ft./sec. for the superflow fan at its design point. This was felt to be too high from a standpoint of mechanical stress.

3.2 DESCRIPTION OF CONCEPT AND CANDIDATE FAN DESIGN

The supersonic fan considered in this study consists of a single stage comprising a rotor and stator. The concept is similar in principle to a supersonic compressor, but it differs by having a stator which removes swirl from the flow without producing a net rise in static pressure. In the present application the goal is to create a stage with a larger velocity at the exit of the stator than at the entrance to the rotor, and thus has an exit static pressure lower than the inlet static pressure. This is possible because at supersonic flight conditions, the flow entering the fan has been decelerated by the inlet and is thus at a higher static pressure than the free stream. Therefore, it is possible to have a fan stage which permits a static pressure drop across the stage without having the pressure drop below atmospheric. Such a stage imparts lower local pressure gradients at the trailing edge of blade suction surfaces, and therefore it is expected that trailing edge separation can be more readily prevented. By keeping the flow attached and wakes small, it is expected that two major sources of losses which accounted for poor performance in many early attempts at supersonic compressors can be diminshed.

Three sources of losses occur in a fully supersonic fan. The first two of these are related to shocks and viscous losses occuring within the passages. These are well recognized from experience with rotors with supersonic relative flow over part of

their radius.

The third type of loss takes place at the entrance of a blade row placed downstream of another. Because one row of blades is rotating with respect to another, the downstream row receives a flow which is non-uniform and is thus unsteady. The result of this unsteadiness is the generation of time varying pressure waves which absorb energy. For a supersonic stage, this is especially serious as strong shocks may form, causing substantial losses. Additionally, this unsteadiness is a source of noise. Therefore, in the design of a supersonic fan stage effort must be made to minimize the magnitude of this unsteady component.

A fan total pressure ratio of 2.8 has been specified at the supersonic cruise point at Mach 2.7. At this flight condition, the axial Mach number at the fan face is 2.2 and the chosen tip tangential Mach number is 1.26, corresponding to a physical tip speed of about 1375 ft./sec. The fan rotor diameter is 7.9 ft. A set of velocity triangles at the mid-blade radial station r/r_{TIP} =0.8 is sketched in figure 3.3. A polytropic exponent of 0.85 was assumed for the stage and the turning required calculated from the Euler Turbine Equation. The impulse type rotor turns the flow about 50 degrees in rotor fixed coordinates, and about 43 degrees of turning are required in the stator to remove swirl from the rotor exit flow.

The requirement for large amounts of turning in both rotor and stator came about from the desire to achieve the specified pressure ratio in a single stage at a reasonable rotor speed.

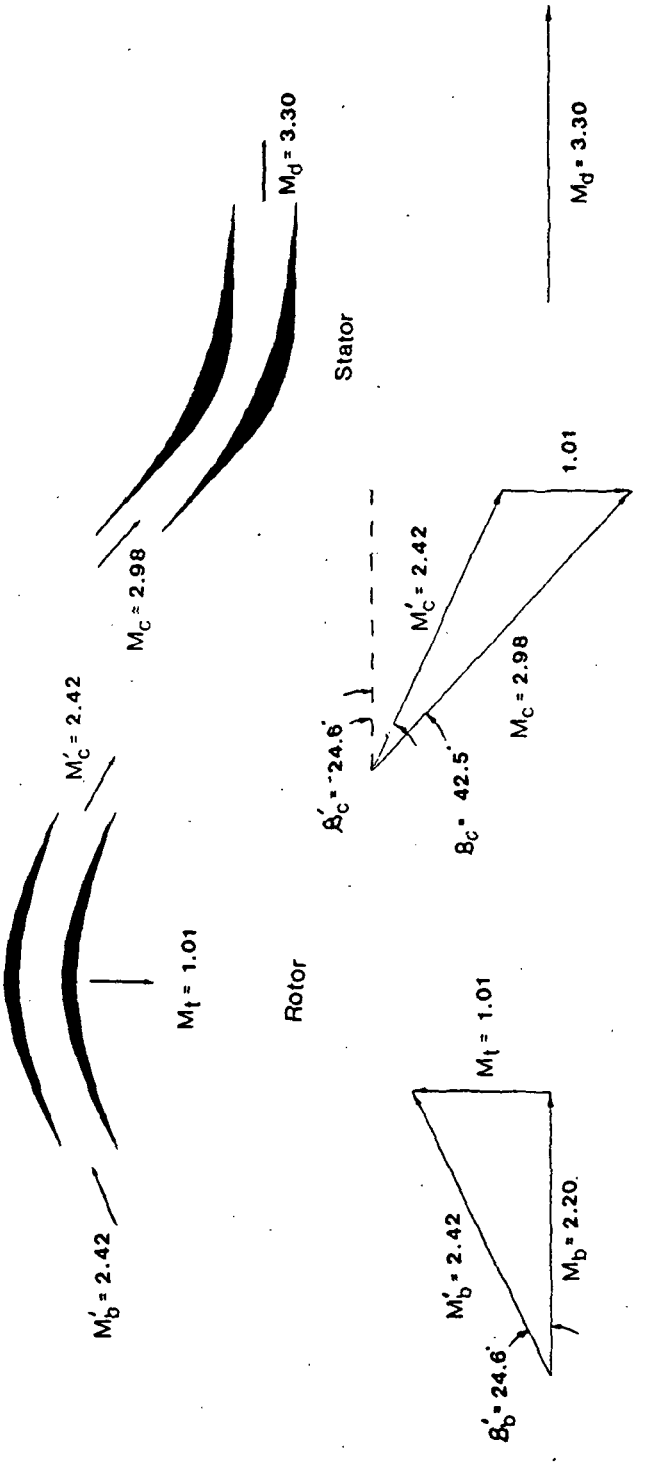

Figure 3.3 Velocity diagram at mid-blade radial station for fan stage.

This places emphasis on the need for careful blade passage design to prevent large shock losses, choking of the flow, and large velocity non-uniformities at the blade exit flow. Operation of the fan stage at supersonic axial Mach numbers gives rise to unique operating conditions. These are:

1. During supersonic operation the flow condition at the fan face are set by the inlet. Therefore rotor speed must be matched to the axial flow to prevent large blade incidence angles which could cause the blade passages to unstart,resulting in large shock losses.

2.Blade surface pressure distribution is influenced to a large extent by wave interaction within the passages. This interaction must be carefully tailored to maintain fully supersonic flow and to produce uniform exit flow.

Candidate rotor and stator mid-blade passage geomtries are presented in Figure 3.4. The rotor cascade has a camber angle of 49.2 degrees and a solidity of 5.9. The blades are 3.0 % thick. The stator has a camber angle of 42.5 degrees and a solidity of 5.6. The blades are 7.4% thick.

The blade shapes were determined by the use of an analytical method which generates surfaces which produce a supersonic vortex flow given the inlet and exit Mach numbers, and the peak values of the Mach numbers on the suction and pressure surfaces. This type of cascade is discussed in more detail in Section 3.4.4.

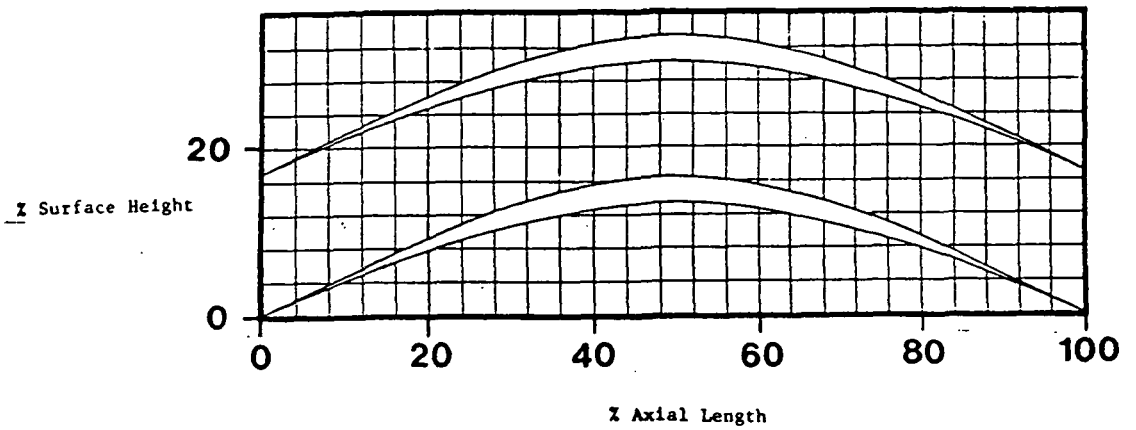

Rotor Cascade Coordinates

% Axial Length	% Surface Height		
	Upper	Lower	Lower + Gap
0	0.00	0.00	16.87
4	1.82	1.75	18.62
8	3.65	3.41	20.28
12	5.48	4.97	21.84
16	7.32	6.41	23.28
20	9.15	7.74	24.61
24	10.86	8.95	25.82
28	12.32	10.04	26.91
32	13.55	11.01	27.88
36	14.57	11.85	28.72
40	15.41	12.57	29.44
44	16.04	13.07	29.94
48	16.36	13.32	30.19
52	16.36	13.32	30.19
56	16.04	13.07	29.94
60	15.41	12.57	29.44
64	14.57	11.85	28.72
68	13.55	11.01	27.88
72	12.32	10.04	26.91
76	10.86	8.95	25.82
80	9.15	7.74	24.61
84	7.32	6.41	23.28
88	5.48	4.97	21.84
92	3.65	3.41	20.28
96	1.82	1.75	18.62
100	0.00	0.00	16.87

Figure 3.4 Rotor and Stator Cascade Coordinates.

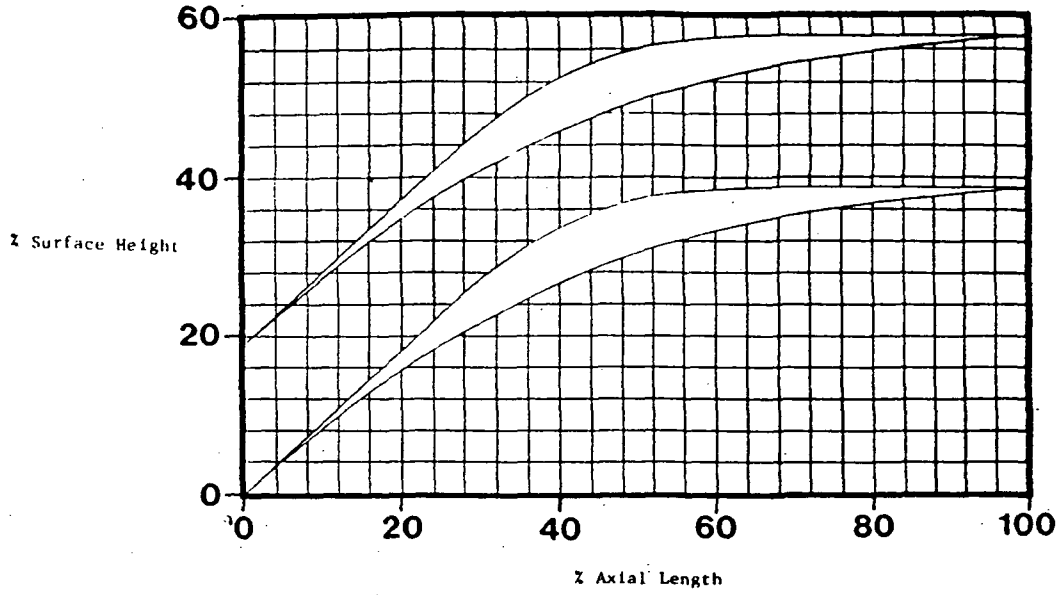

Stator Cascade Coordinates

% Axial Length	% Surface Height		
	Upper	Lower	Lower + Gap
0	0.00	0.00	19.26
4	3.68	3.54	22.80
8	7.35	6.91	26.17
12	11.01	10.09	29.35
16	14.67	13.09	32.35
20	18.33	15.91	35.17
24	22.00	18.50	37.76
28	25.61	20.91	40.17
32	28.88	23.12	42.38
36	31.58	25.13	44.39
40	33.86	26.96	46.22
44	35.61	28.70	47.96
48	36.95	30.11	49.37
52	37.88	31.88	50.64
56	38.51	32.64	51.90
60	38.86	33.77	53.03
64	39.12	34.65	53.91
68	39.17	35.42	54.68
72	39.19	36.07	55.33
76	39.19	36.67	55.93
80	39.19	37.27	56.53
84	39.19	37.84	57.10
88	39.19	38.20	57.46
92	39.19	38.52	57.78
96	39.19	38.86	58.12
100	39.19	39.19	58.45

Figure 3.4 (cont.) Rotor and Stator Cascade Coordinates.

3.3 APPROACH TO DESIGN AND DESIGN GOALS

Little precedent exists for blade shapes, velocity triangles, or passage velocity distributions for a supersonic fan. Therefore, effort must be made to gain insight into the requirements for a supersonic fan stage. The thrust of this investigation was to gain appreciation for conditions under which fan must operate, establish flow turning angles, and come up with a design of candidate blade passages. To simplify the problem within the context of this investigation, the blade design study was confined to operation at the design point and the problem reduced to design of two dimensional cascades which would represent a candidate fan at its mid-blade radial station.

Fan turning was established by choosing fan tangential Mach number, assuming a fan stage polytropic efficiency consistent with the system study, and then establishing turning by use of the Euler Turbine Equation for the needed stage total temperature ratio.

The choice of a supersonic vortex velocity distribution within the blade passages allowed analytical calculation of blade geometries. (See References 8 & 9.)

Once a blade design was generated, a 2-D Euler equation solver was used to obtain a detailed picture of the flow within the passages. This was done for the rotor and stator at design Mach numbers and incidence angles, and for the rotor cascade flow solutions were calculated for a variety of flow incidence angles

and Mach numbers. A simple loss analysis was performed using the Lieblein correlation for cascade data. The following design criteria were set for the cascade passages:

1. Wave losses due to rotor-stator interaction must be minimized. To facilitate this rotor blade passages must be designed to perform flow turning of the amount required for a stage pressure ratio of 2.8 and provide uniform exit profile at design Mach number and incidence angles. It is also important to achieve reasonably uniform exit flow from the stator. This is to prevent large shock and viscous mixing losses downstream of the stator.

2. The flow diffusion factor must be low enough that flow is expected to remain attached, and the total pressure loss coefficient as predicted by the Lieblein method must be low enough that cascade profile losses are consistent with the requirement of a stage polytropic efficiency of 0.85.

3. Shocks must be minimized within the blade passages. This is important for two reasons, the first of which is to minimize the total pressure loss directly associated with the formation of shocks. The second reason is to prevent excessive growth of the wake momentum thickness due to interaction between shock waves and blade boundary layers. Hence, in the cascades designed in this investigation, the leading edges have been made thin and sharp.

3.4 FAN AERODYNAMICS

Before moving on to the discussion of the blades designed in this investigation, it is useful to discuss some fundamental points. In the following sections, the operating conditions unique to an axially supersonic blade row are addressed, as are considerations for designing blades which can produce large turning, while maintaining supersonic flow throughout the passages and achieving uniform flow at the blade exit stations.

3.4.1 DISCUSSION OF STEADY FLOW AT THE ENTRANCE OF A CASCADE FOR SUPERSONIC AXIAL VELOCITY

Consider a supersonic cascade having blades of zero thickness and without camber as shown in Figure 3.5. The incident flow is supersonic steady and has an axial component that is subsonic and of magnitude OB. For steady conditions no waves can travel upstream of the infinite cascade as explained in Reference 7. Therefore, the velocity denoted by the vector OA in front of the cascade must be parallel to the blades.

From this argument, it follows that if the tangential velocity AB is increased to A_1B_1, for steady flow to prevail the axial velocity OB increases correspondingly to OB_1 such that the flow remains aligned with the blades. This remains true for a decrease or increase in tangential velocity only up to the point

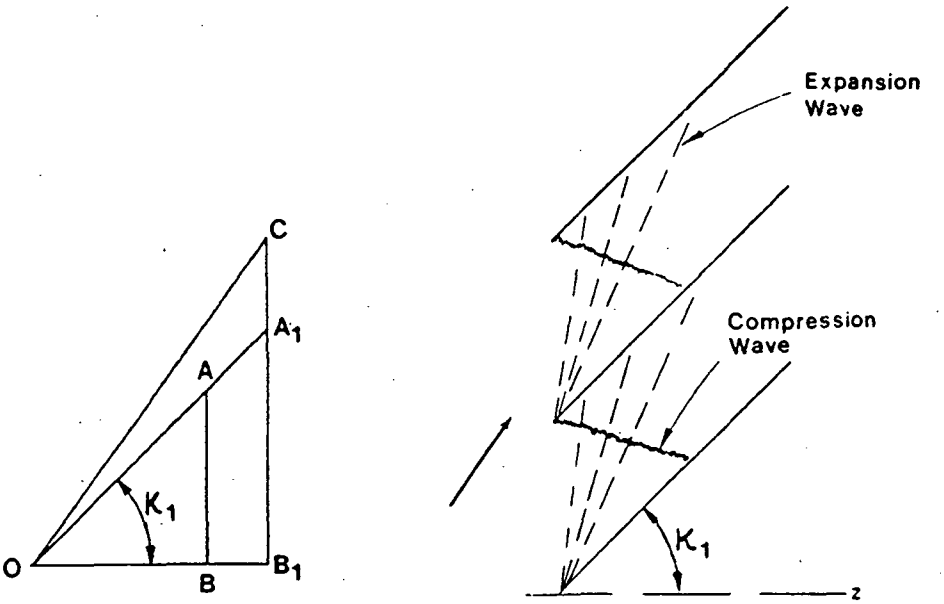

a. Variation of tangential velocity.

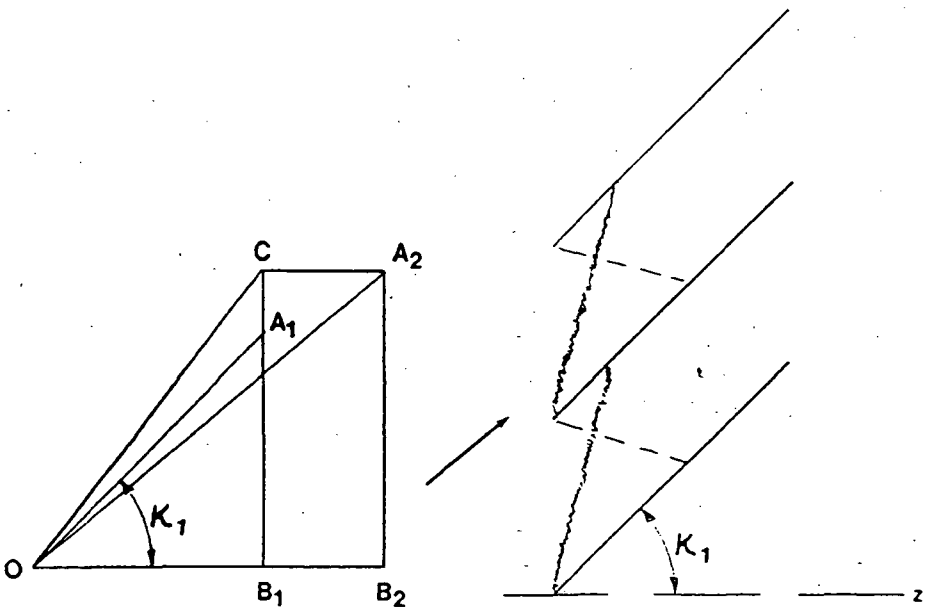

b. Variation of axial velocity.

Figure 3.5 Flow at entrance of supersonic cascade having zero thickness and camber. (from Ref. 7)

at which the axial velocity becomes sonic.

At the point where the axial velocity becomes sonic the situation changes qualitatively for the following reason: If tangential velocity is increased infinitesimally, waves of infinitesimal strength will be produced at the leading edge. However, these will be contained within the passage. Only by production of a shock of finite strength could waves be propagated upstream. Such a shock would in turn produce flow with a subsonic axial component. Suppose now, with the axial velocity sonic, that the tangential velocity is increased from A_1B_1 to B_1C. This presents a relative velocity which increases from OA_1 to OC. This produces an incidence angle between the flow and the blades. Expansion waves are produced on the trailing surfaces of the blades. These are contained within the passages as are the compression waves as long as the compression waves are not of sufficient strength to produce shock detachment. Thus no waves are transmitted upstream and the axial velocity is unchanged. This situation represents a steady state and it follows from this argument that the maximum axial Mach number that can be produced by increasing the tangential velocity is sonic.

Consider now a case wherein the axial velocity is varied. When the axial velocity OB is less than sonic, an increase of axial velocity produces a change in the direction of the axial velocity OA relative to the blades. Unsteady waves are produced at the leading edges of the blades. These move upstream and reduce the axial velocity to the original value OB. However, the

situation is different if the axial component is greater than or equal to sonic.

Suppose initially, the velocity is represented by the triangle OB_1C with the axial component OB_1 . (See Fig. 3.5) A small increase takes place which increases the axial component form OB_1 to OB_2 and the relative velocity is thus represented by OA_2 and this time, a compression wave is produced on the trailing surface of the blade and expansion waves are generated by the leading surface. The expansion waves are of course contained within the passage. If the compression waves are sufficiently weak, (a sufficiently weak shock being one in which the axial component of the flow behind the shock is supersonic), and if the shock detachment angle is not exceeded,then the compression wave will be contained within the passage. Since there is no upstream influence exerted by these waves, this represents a steady condition. This shows how the cascade may attain operation with supersonic axial Mach number, and that this can only be attained by change of the flow Mach number upstream.

These considerations for the infinite cascade may be extended to the superonsic rotor with the following implications: If the entrance region to the blades is straight, the velocity relative to a rotor with subsonic axial velocity is not changed in direction but tends to remain aligned with the blade suction surface. A change in tangential velocity of the rotor will produce a corresponding change in the axial velocity of the flow up until the condition of the flow becoming axially sonic. Below this point the axial velocity at the fan face is influenced by

the rotational speed of the rotor and is therefore independent of flight conditions.

Once the axial component of the velocity has become supersonic, an increase of the rotational speed of the rotor can produce no change in the axial velocity, and the mass flow is fixed by the inlet. The fan may then operate at different mass flows and pressure ratios at the same rotational speed. This discussion may be extended to a blade with a finite leading edge thickness to consider the effects of the leading edge on the flow.

3.4.2 FLOW ANGLE RESTRICTIONS ON AN AXIALLY SUPERSONIC CASCADE WITH THICKNESS

Consider the entrance region of a supersonic cascade. Assume that downstream of the entrance region the blade geometry is such that fully supersonic flow is permitted. The geometry of the entrance region comprises a wedge of half angle δ which is inclined such that the trailing surface AB is inclined at an angle $K_1 + \delta$ from the axial direction. The axial component of the incident flow is supersonic.

First assume that the flow is such that $\beta_1 \geq K_1 + \delta$. Expansion waves form on the trailing surface but are completely contained within the passage since the axial Mach number is greater than 1. On the leading surface AC, the flow undergoes a compressive flow deflection of magnitude $\Theta = \beta_1 - K_1 + \delta$. If the flow deflection is small enough that for the incident Mach number M_1 the flow is below the angle which will cause shock detachment, an oblique shock contained within the passage results, and there is no upstream influence. If however the flow deflection is large enough to cause shock detachment, the flow behind the shock is subsonic and the passage unstarts.

Next consider the case where $\beta_1 < K_1 + \delta$. In this case, a compression wave is generated by surface AB as shown in Figure 3.6. Assume however, that δ is small enough that an attached compression wave forms on AC if $\beta_1 > K_1 - \delta$. Otherwise, if

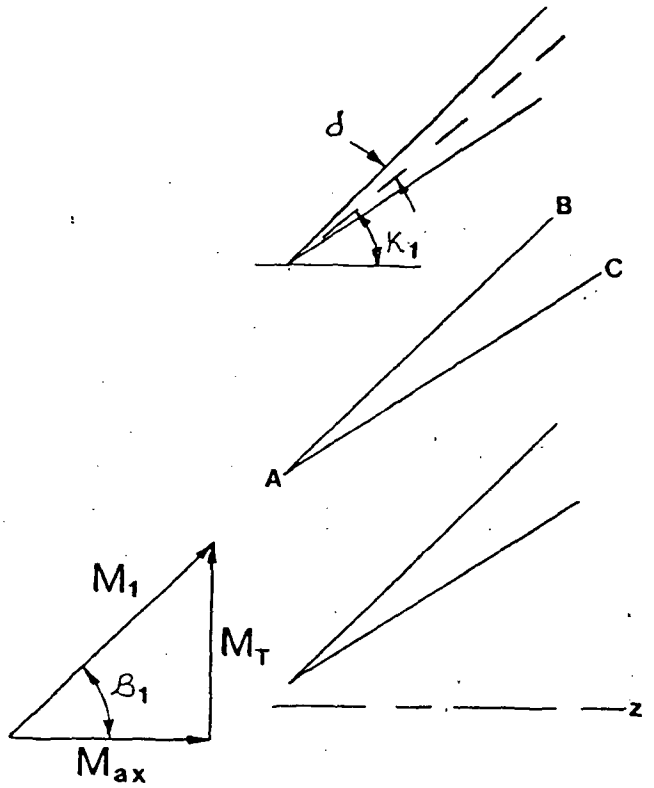

Cascade entrance region geometry and flow notation.

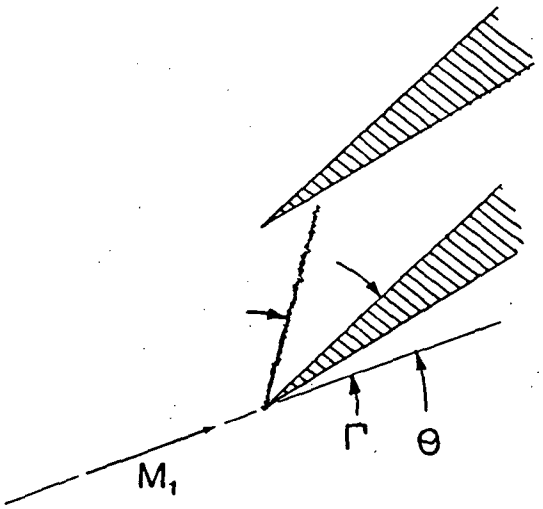

Shock wave notation.

Figure 3.6 Flow in axially supersonic cascade with straight entrance region.

Figure 3.6 (cont.) Flow in axially supersonic cascade with straight entrance region.

$\beta_1 < \kappa_1 - \delta$ expansion waves form on the leading surface AC. In either case, waves from the leading surface are contained within the passage and exert no upstream influence.

Three scenarios are possible:

1. Flow deflection angle $\theta = \kappa_1 + \delta - \beta_1$ is large enough to cause shock detachment and the passage unstarts in a similar fashion to the case of a detached shock forming on the leading surface.

2. θ is small enough to allow an attached oblique shock to form and the shock wave angle relative to the incident flow angle is such that $\Gamma < 90^\circ - \beta_1$. In this case the shock is contained within the passage and no waves are propagated upstream.

3. A third possibility exists that under certain conditions the flow deflection angle while producing an attached shock on an isolated wedge produces flow downstream of the shock with a subsonic axial component. The associated shock angle is such that $\Gamma > 90^\circ - \beta_1$. In this case the shock points upstream. Clearly this is inconsistent with the condition of axially supersonic flow and the passage unstarts. Depending on choice of geometry of the entrance region and Mach number, this condition of the wave pointing upstream may not occur below the angle at which the shock would become detached.

This discussion based on 2-D considerations places

restrictions on the range of incidence angles over which a blade row may operate in the axially supersonic condition. These restrictions are derived independently of the details of the blading geometry downstream. It should be pointed out however, that choking may occur inside the passage at incidence angles below which this may be a problem, and hence should not be taken as conservative estimates of the allowable range of blade incidence angles.

3.4.3 THE IMPORTANCE OF WAVE INTERACTION IN BLADES WITH LARGE TURNING

Since it has been proposed to incorporate blade passages in the design which are fully supersonic, it is useful to model the cascade as a series of stacked supersonic nozzles rather than airfoils. Since the flow is supersonic throughout, there can be no communication between suction and pressure surfaces of a single blade, (except through boundary layers but this is neglected in this inviscid analysis), yet strong interactions may be present between adjacent blades. These are indeed necessary to provide desired flow conditions. If the blades were spaced such that no interaction took place, and if the blade surfaces were shaped such that no strong shock waves were generated, the Mach number of the flow on the concave surface would decrease in a Prandtl-Meyer compression. Likewise, the flow on the convex surface would increase in Mach number in a Prandtl-Meyer expansion. At the trailing edge of the blade, the flow on the concave surface would have its Prandtl-Meyer angle decreased by the value of the turning angle, while the flow along the convex surface would have its Prandtl-Meyer angle increased by the value of the turning angle. Hence in blade passages where turning is large, the velocity discontinuity at the trailing edge would be considerable.

A second problem arises in the case where the compressive turning angle is greater in magnitude than the Prandtl-Meyer angle of the incident flow. In this case, the Mach number on the

concave surface would fall below 1 in conflict with the design requirment.

Thus, it is clear that blade passage geometry must provide for wave interaction to achieve the desired passage Mach number distribution. However, in tailoring passage geometry, care must be taken to insure that the resulting shapes stack to form closed blades of positive thickness.

3.4.4 THE SUPERSONIC VORTEX BLADE

The design of supersonic blade sections described herein is based on establishing a vortex flow within the blade passages, as developed in References 8 and 9. The blade so designed consists of three major parts; inlet transition arcs, circular arcs, and outlet transition sections. A representative passage is shown in Figure 3.7. The inlet transition arcs are required to convert the uniform parallel flow at the leading edges into a vortex flow. The circular arcs maintain the vortex flow field, thereby continuing flow turning. The outlet transition arcs restore the flow to parallel flow at uniform Mach number at the blade exit. Additionally, on the blade suction surfaces, straight line sections are used to close the blade formed by the passages.

A typical blade surface Mach number distribution is shown in Figure 3.8. This shows that the inlet transition section on the concave surface reduces the Mach number from its inlet value M_1, to a preselected value of the value of the pressure surface Mach number M_L. Likewise, the transition arc on the convex surface increases the inlet Mach number to the specified value for the upper surface M_U. The Mach numbers remain at a constant value on the circular arc surfaces. At the outlet transition arcs, the flow on the surfaces is returned to a uniform flow at the prescribed exit Mach number M_2.

The flow turning produced by either the upper or lower surface consists of two parts; that which is produced by the

AB	Inlet suction surf. transition arc
FG	Outlet suction surf. transition arc
CD	Inlet pressure surf. transition arc
HI	Outlet pressure surf. transition arc
AF	Suction surf. circular arc
CH	Pressure surf. circular arc
BE and GJ	Straight lines

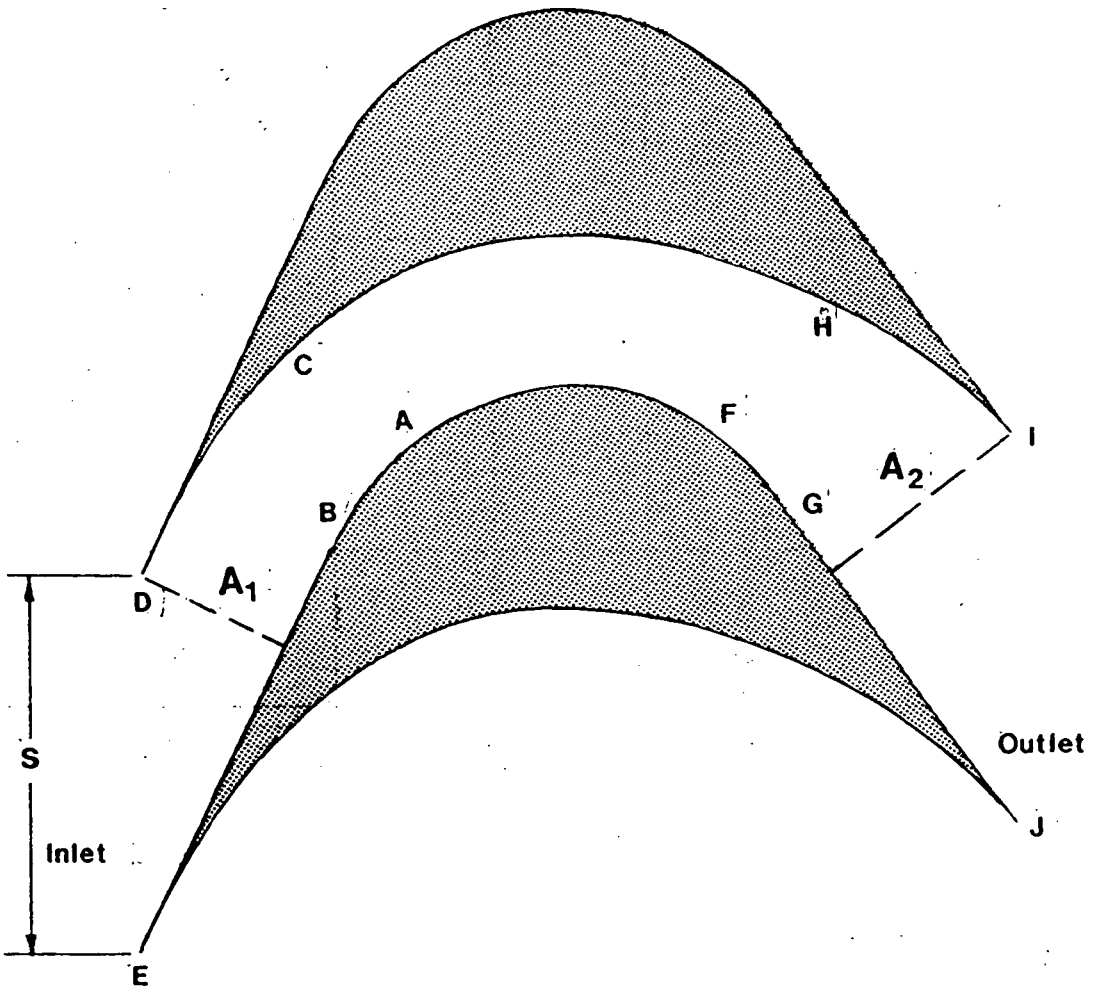

Figure 3.7 Geometry of supersonic vortex type blade sections.

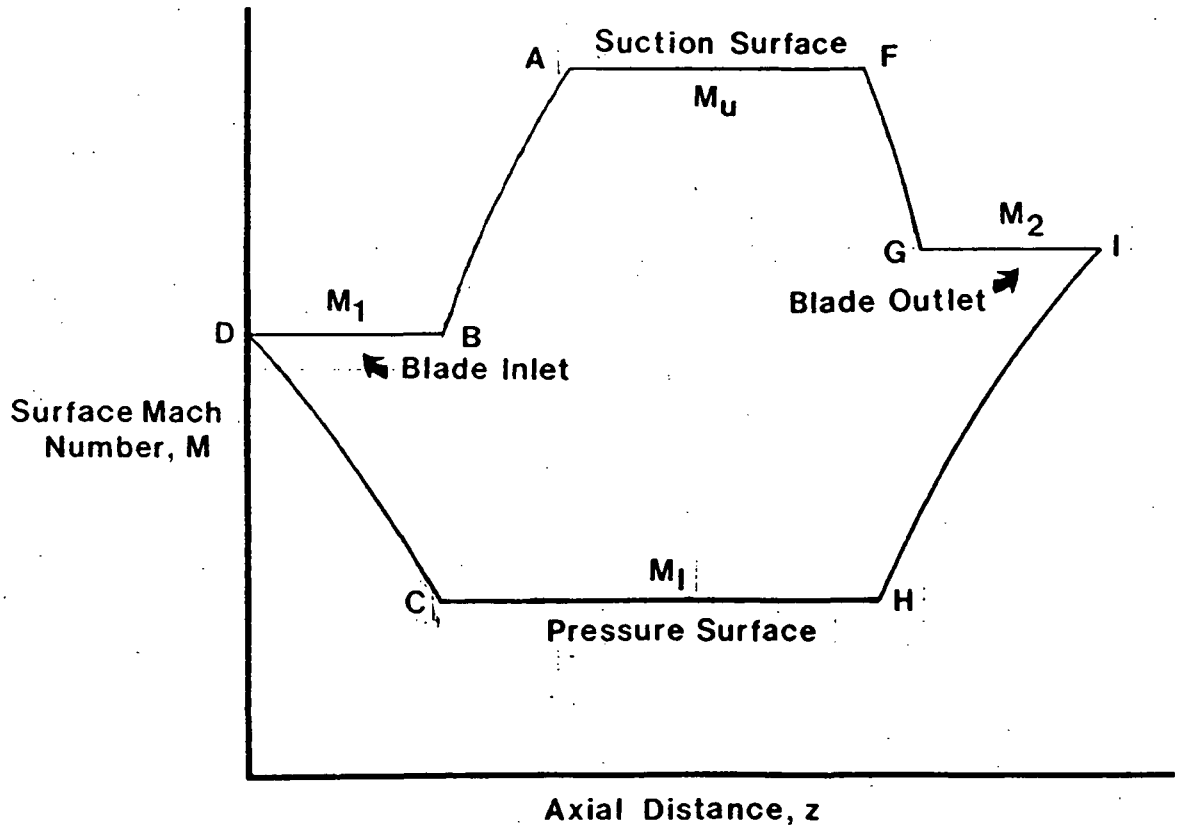

Figure 3.8 Surface Mach number variation for typical blade section at design point.

transition arcs, and that which is produced by the circular arcs. Since the flow is assumed to be isentropic and fully supersonic, it is convenient in this case to introduce description of the flow in terms of its Prandtl-Meyer angle.

The characteristic lines of the flow through a supersonic vortex blade passage is shown in Figure 3.9. It can be seen that the surfaces of the inlet tranistion arcs are boundaries of simple regions (i.e. no wave interaction takes place in this region.) Thus, the change in the Prandtl-Meyer angle of the flow on the passage surfaces is equal to the difference in angle between the surface and the inlet flow. The Mach number distribution in the exit transition region is identical to that in a similarly shaped inlet region in which the direction of flow has been reversed. (This is due to flow reversal properties in isentropic supersonic flow.) Hence, the turning angle required of the transition arcs is given by $\nu_1 - \nu_u$ and $\nu_1 - \nu_L$ for the upper and lower inlet tranistion arcs, and $\nu_2 - \nu_u$ and $\nu_2 - \nu_L$ for the upper and lower exit transition arcs. Hence, it can be reasoned that the maximum suction surface, and minimum pressure surface Mach numbers are limited by the relations:

$$\nu_u \leq \nu_1 + \frac{\beta_2 - \beta_1}{2}$$

$$\nu_L \geq \nu_1 - \frac{\beta_2 - \beta_1}{2}$$

For a 2-D section, the flow exit angle and the exit Mach number have a unique relation for the given inlet Mach number and

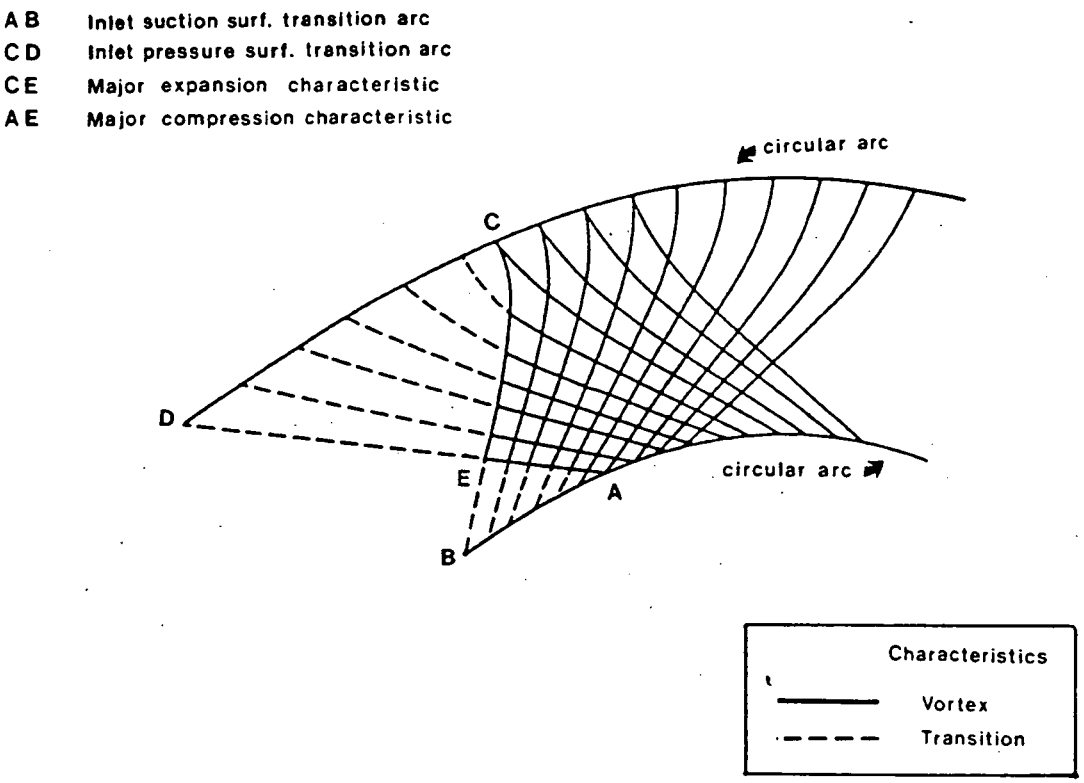

Figure 3.9 Characteristic network within blade passage at design point. (from Ref. 9)

flow angle. To obtain a closed blade, the exit area normal to the flow is given by the relation:

$$\frac{A_2}{A_1} = \frac{\cos \beta_2}{\cos \beta_1}$$

Then to satisfy the continuity equation, the inlet and exit Mach numbers are related by the isentropic one-dimensional relations for a channel of area ratio A_2/A_1.

As stated above, a single flow passage may be constructed for any selection of suction and pressure surface peak Mach numbers, provided that the sum of required transition arc turning does not exceed the total turning angle desired. However, satisfying these conditions does not guarantee that closed blades will result when these passages are in cascade. There are cases where the result would be blades of negative thickness, but for most practical choices of turning angles and Mach numbers, this has not been a problem.

3.5 DESIGN TOOLS

3.5.1 ANALYTICAL DESIGN PROGRAM FOR SUPERSONIC VORTEX BLADES

A FORTRAN computer program for the design of supersonic passages based on establishing a vortex velocity distribution as outlined in Reference 9 was adapted for use on a DEC PDP 11/70 computer. The construction of passages which produce supersonic vortex flow is discussed briefly in Section 3.4.4.

The information required for input consists of inlet flow angle, inlet and flow Mach numbers, and maximum Mach number on suction surface and minimum Mach number on pressure surface. All Mach numbers are specified in terms of their Prandtl-Meyer angles.

The program calculates, by the method of characteristics, the shapes of transition arcs which produce a supersonic vortex flow. The strength of the vortex is determined by prescribing the peak suction and pressure surface Mach numbers. The transition arcs are connected to circular arcs and straight lines are used to form closed blades. The coordinates of these blades are given as output.

3.5.2 2-D EULER FLOW ANALYSIS CODE

The Euler Equation Solver employed in this study is a conservative streamtube solution of the steady state equations. This technique was developed at MIT and is explained in detail in Reference 10. The method is similar to streamline curvature methods but uses a conservative finite volume formulation to ensure correct shock capturing. In this investigation, the supersonic solver was used which employs a space marching solution procedure which takes full advantage of the hyperbolic character of the steady state equations.

The method is quite robust and fast, (typical solution times being on the order of 10 CPU seconds on a DEC PDP 11/70 computer) making it ideally suited for design problems. For design calculations, the method has the additional advantage that flow boundary conditions can be specified in terms of blade passage geometry surface pressure distribution, or combinations thereof. Plotting software for producing streamline diagrams and Mach number contours accompanies the flow solution program.

3.6 DISCUSSION OF FAN CASCADES

3.6.1 FAN CASCADES AT DESIGN POINT

The streamline grids of the rotor and stator cascade, as calculated by the supersonic Euler solver at the design point, are shown in Figure 3.10. Also included are Mach number contours and Mach number profiles of the blade exit flows. The streamlines and Mach number contours of both rotor and stator cascades show the flows in the passages to be shock free.

It must be pointed out that the complete absence of shocks was obtained by generating blade geometries in which the leading edges are infinitely thin. This is unacceptable for structural reasons, in constructing practical blades. A refinement of these cascade designs would be to modify them with a leading edge with a finite wedge angle. A method for doing this is suggested in Reference 8. It is felt that these could be incorporated without drastic changes to the overall blade profiles, and the leading edge compression waves could be effectively cancelled by generating expansion waves downstream. In doing so, the supersonic vortex flow pattern could be maintained.

In constructing blade profiles with the analytical method of characteristics program, rotor suction and pressure surface Mach numbers of 3.1 and 1.9 were specified. The Euler solver calculated peak suction and pressure surface Mach numbers of 2.9 and 1.9 showing excellent agreement with theory. The exit profile shows excellent flow uniformity. In calculating the stator cascade geometry, suction and pressure surface peak Mach

numbers of 4.3 and 2.1 were specified. The peak Mach numbers calculated by the Euler solver are 3.8 and 2.2. Part of the discrepancy may lie in the fact that the analytical routine had difficulty generating a geometry with a 0.0 degree exit angle. As a result, the stator was designed by graphically joining the required inlet transition arcs with exit transition arcs desinged for a non-zero flow exit angle. This may also account for the lack of flow uniformity (around 5% about the mean Mach number) in the stator exit Mach number profile. However, this may not be a serious problem, as long as the nonuniformity does not cause strong shocks to form in the nozzle.

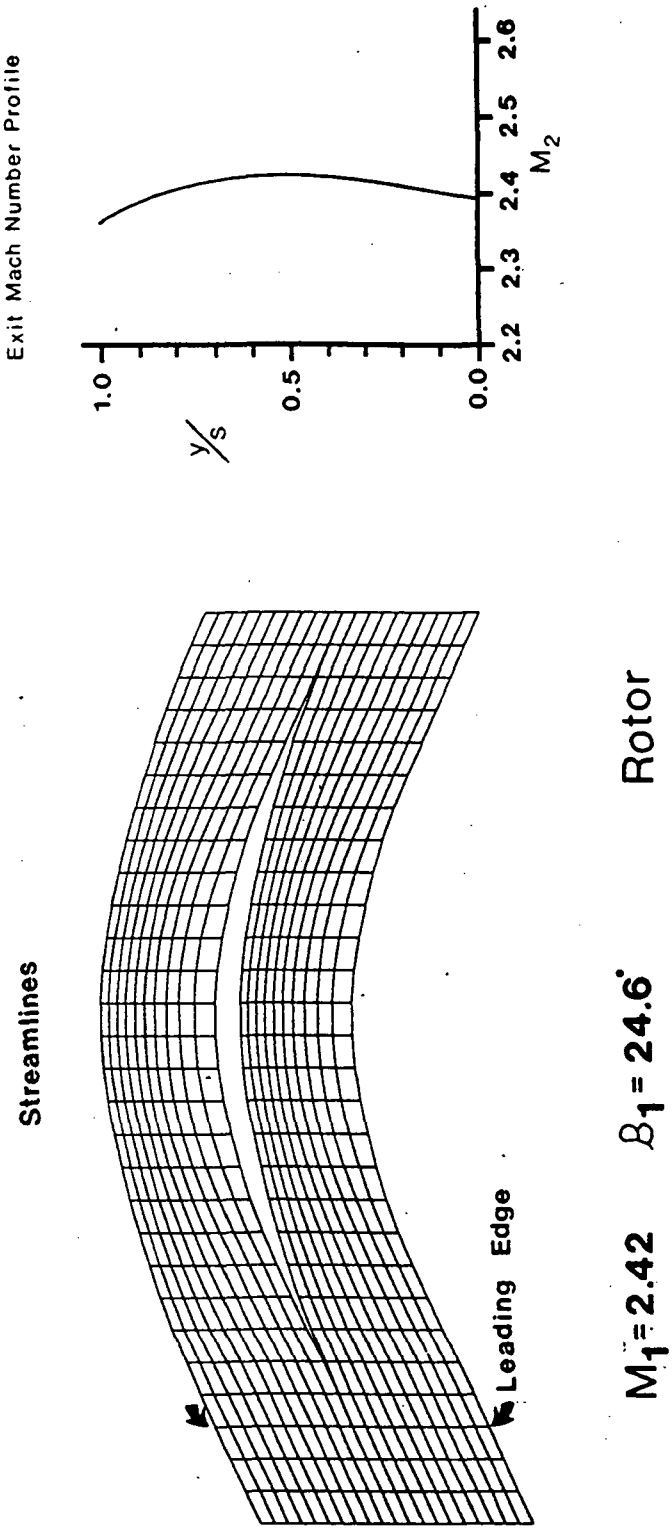

Figure 3.10 Flow through fan cascades at design point.

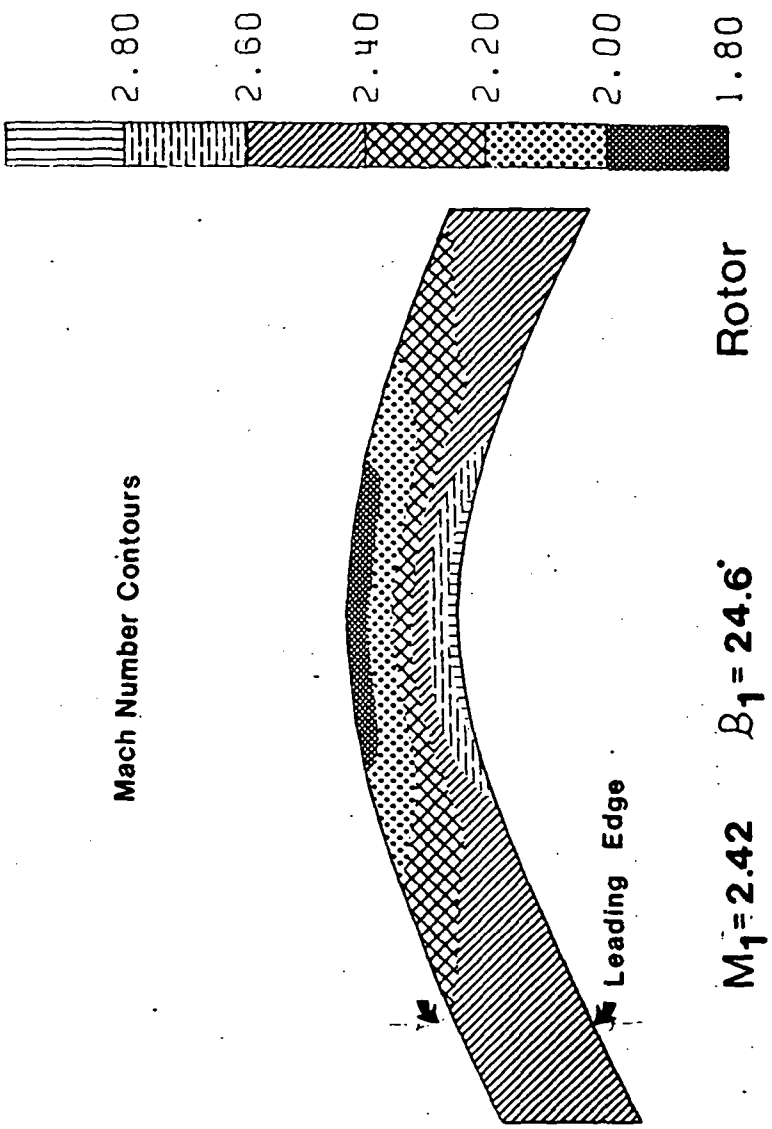

Figure 3.10 (cont.) Flow through fan cascades at design point.

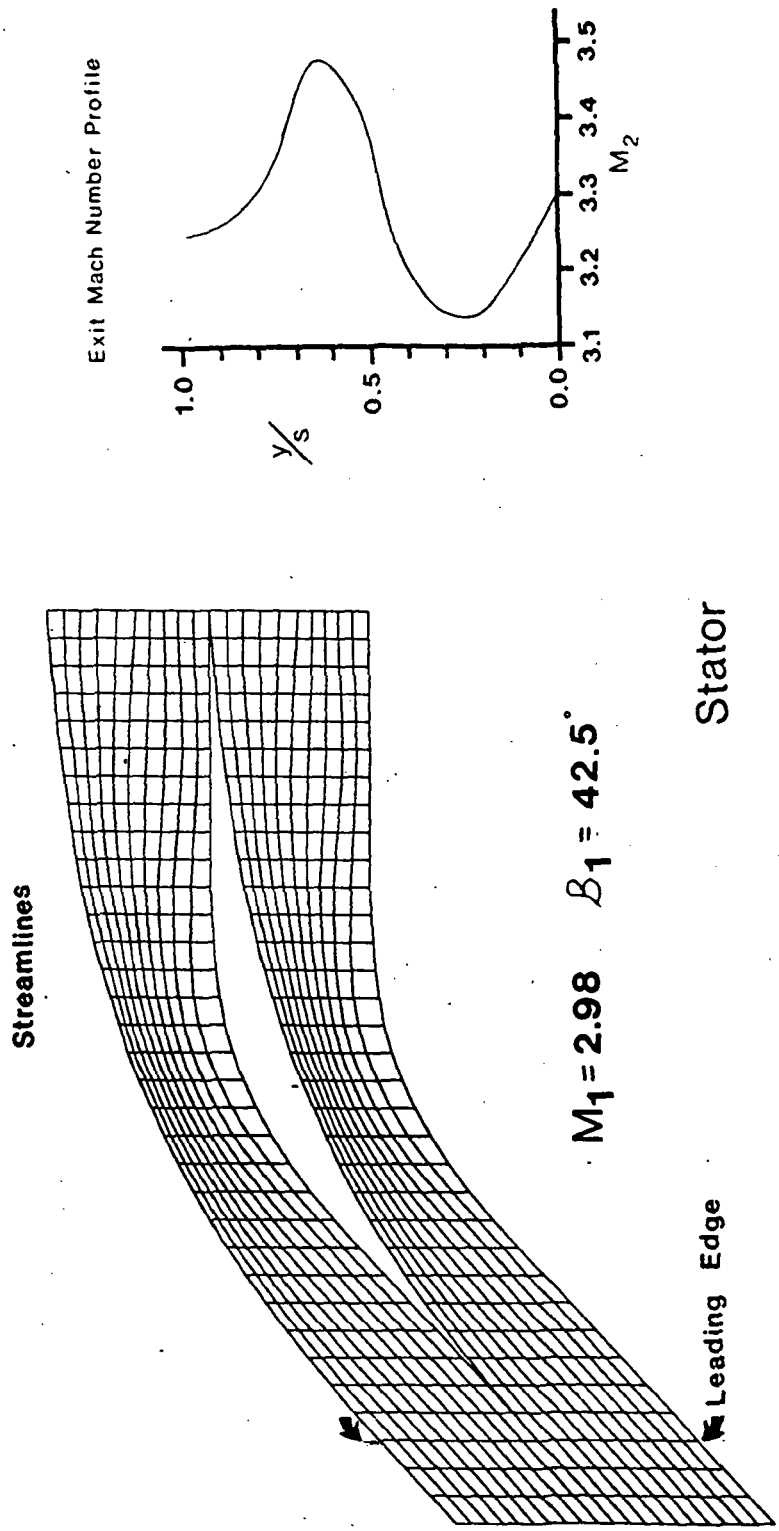

Figure 3.10 (cont.) Flow through fan cascades at design point.

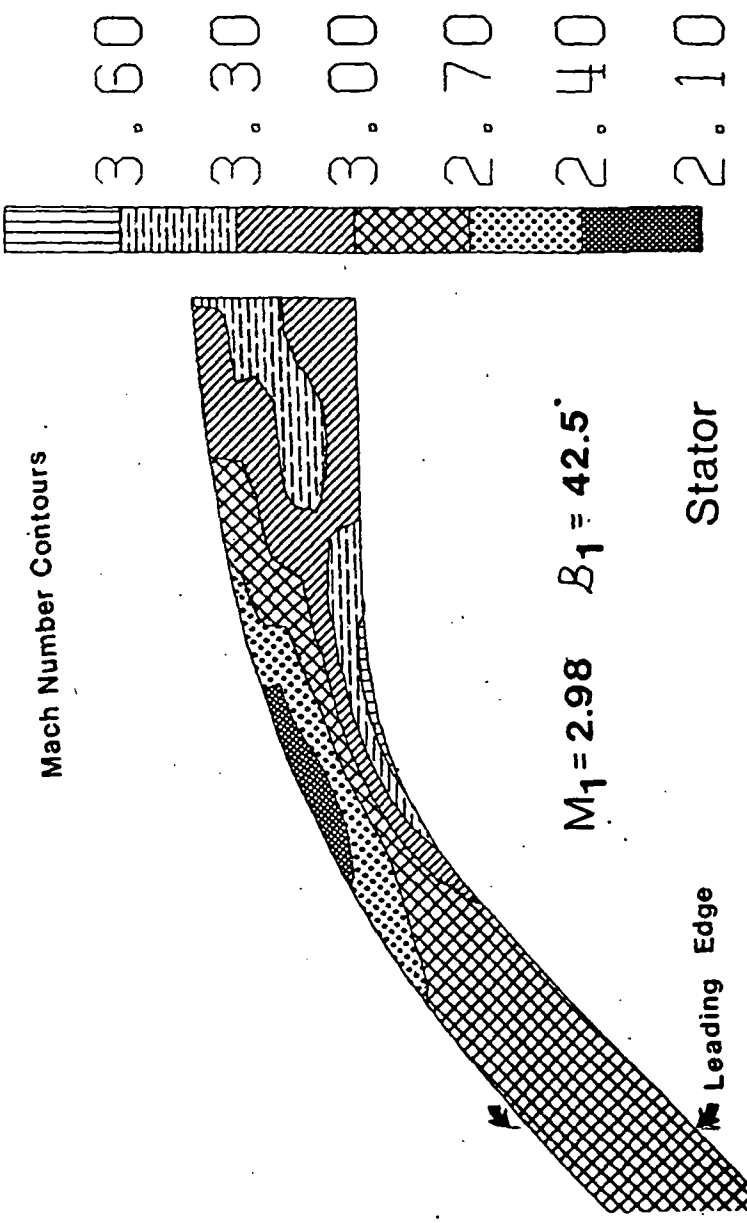

Figure 3.10 (cont.) Flow through fan cascades at design point.

3.6.2 ESTIMATION OF PASSAGE LOSSES

The Lieblein correlation of cascade data was used to estimate passage losses at the design point. While this method was derived using low speed cascade data, limited data on fully supersonic cascades suggests applicablility of the method to blading of this type at least over a range of incidence angles where shock losses are small.

LaRocca investigated 2 annular cascades incorporating 36 degrees of turning at an inlet Mach number of 2.0. One passage incorporated no static pressure rise across the blade row, while the second featured a slight static pressure drop. The solidity ranged from about 4.1 at the tip to 5.2 at the hub. For these cascades, the measured total pressure loss coefficient was about 1% higher than that predicted from correlation with the diffusion factor. A possible source of the additional loss are unaccounted for shock losses. (See Reference 14.)

It is expected that there are limits outside which extrapolation of loss data to high Mach number blading will be in considerable error. This would be in situations where strong waves occur in the passages. Interaction between shock waves and blade surface boundary layers can substantially alter the behavior of the boundary layer from that observed in flows where there are no shocks present. Therefore, in applying the Lieblein correlation to supersonic blading this phenomenon must be taken into account.

For the cascade passages presented for the supersonic fan, with sharp leading edges and pressure distributions tailored to eliminate strong waves at the design point, it is expected that at the design point the Lieblein correlation is adequate for a first estimate of passage losses.

The loss calculation was carried out according to the method presented in Reference 13. First the local diffusion factor was calculated according to:

$$D_{loc} = \frac{V_{max} - V_2}{V_{max}}$$

and the momentum thickness ratio of the wake taken from Figure 3.11 The using the relation:

$$\bar{\omega} = 2\left(\frac{\theta^*}{c}\right)\frac{\sigma}{\cos\beta_1}\left(\frac{\cos\beta_1}{\cos\beta_2}\right)^2$$

the loss coefficient was calculated.

For the rotor, the diffusion factor D_{loc} is 0.10 yielding a blade momentum thickness ratio of about 0.005. The total pressure loss coefficient of the rotor cascade is thus 0.065. The stator cascade across which there is a static pressure loss, has a very low diffusion factor of 0.02. The wake momentum thickness ratio is again on the order of 0.005 and the total pressure loss coefficient is about 0.030.

The low diffusion factors and hence relatively thin momentum thicknesses of the boundary layers of both rotor and stator cascades suggest that both boundary layers are attached at the

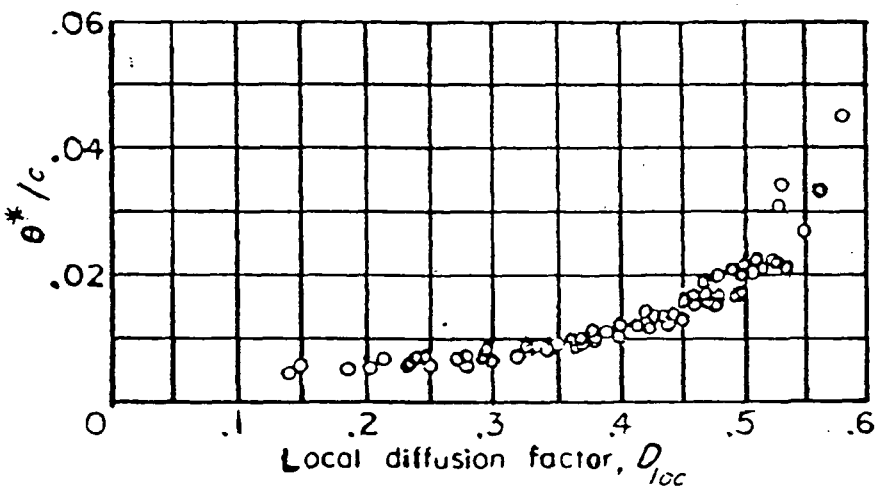

Figure 3.11 Correlation of wake momentum thickness ratio with local diffusion factor at reference incidence angle. Based on NACA low-speed-cascade data. (from Reference 13.)

design point and there is some margin before separation is likely to occur. Suction surface boundary layers, for subsonic blading at least, remain attached up to diffusion factors of around 0.5 where the momentum thickness is seen to increase rapidly, thereby suggesting that separation has occurred.

The adiabatic efficiency of a stage made up the rotor and stator cascades, accounting for the losses estimated above was calculated according to the formula:

$$\eta_{stage} = 1 - \frac{\left\{\frac{\gamma-1}{\gamma}\right\}\left\{\tilde{\omega}_b'\left[1-\frac{P_b}{P_{tb'}}\right]+\tilde{\omega}_c\left[1-\frac{P_c}{P_{tc}}\right]\right\}}{\tau_{stage}-1}$$

from Reference 3. The adiabatic efficiency predicted from this calculation is 0.94 corresponding to a polytropic exponent for the stage of about 0.95.

This is at best an incomplete analysis of losses that might be present in a fan stage made up of these cascades as three dimensional and endwall effects, and rotor-stator interaction losses have not been estimated. However, it does serve to illustrate that the cascade geometries presented allow a margin of about 0.10 for other types of losses in designing a fan stage with a polytropic efficiency of 0.85, as assumed in Chapter 2.

3.6.3 FAN ROTOR CASCADE WITH FLOW MISALIGNMENT

With the axial Mach number set at 2.2, the rotor blade incidence angle was varied in 5 degree increments. This simulates conditions at the fan face when the flight Mach number is 2.7, and the rotor tangential speed is varied from that value which produces flow at zero incidence. Convergence of the Euler solver was obtained for incidence angles varying from -10 to +5 degrees. This suggests that axially supersonic flow can be maintained over a range of at least 15 degrees at this flight condition. Streamline grids and exit Mach number profiles are shown for these cases in Figure 3.12. It is believed that this represents a fairly conservative estimate of allowable incidence angles, since the supersonic flow solver fails to converge whenever a grid point is encountered where the axial component of the Mach number falls below 1. Even if axially supersonic flow breaks down, this analysis does not suggest any particular problems with operating in an axially subsonic condition. However, a transonic flow solver would be required to study this in further detail.

As expected, shocks are observed in the passages. These are relatively weak and it is not expected that they are sources of major losses in themselves. However, as pointed out in the previous section, their effect on the boundary layer may lead to larger blade wakes.

Additionally changing incidence angle leads to

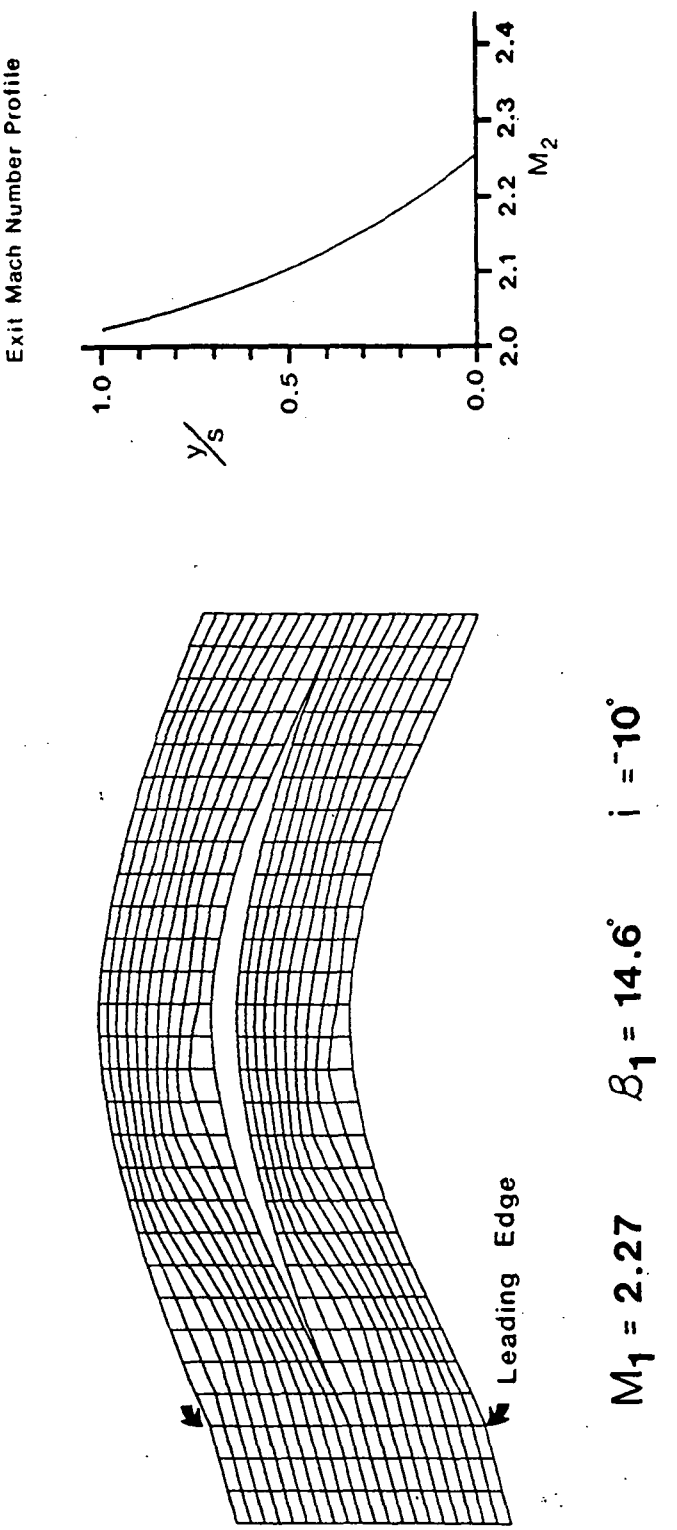

Figure 3.12 Effect of incidence angle on flow in rotor cascade with axial Mach number 2.2.

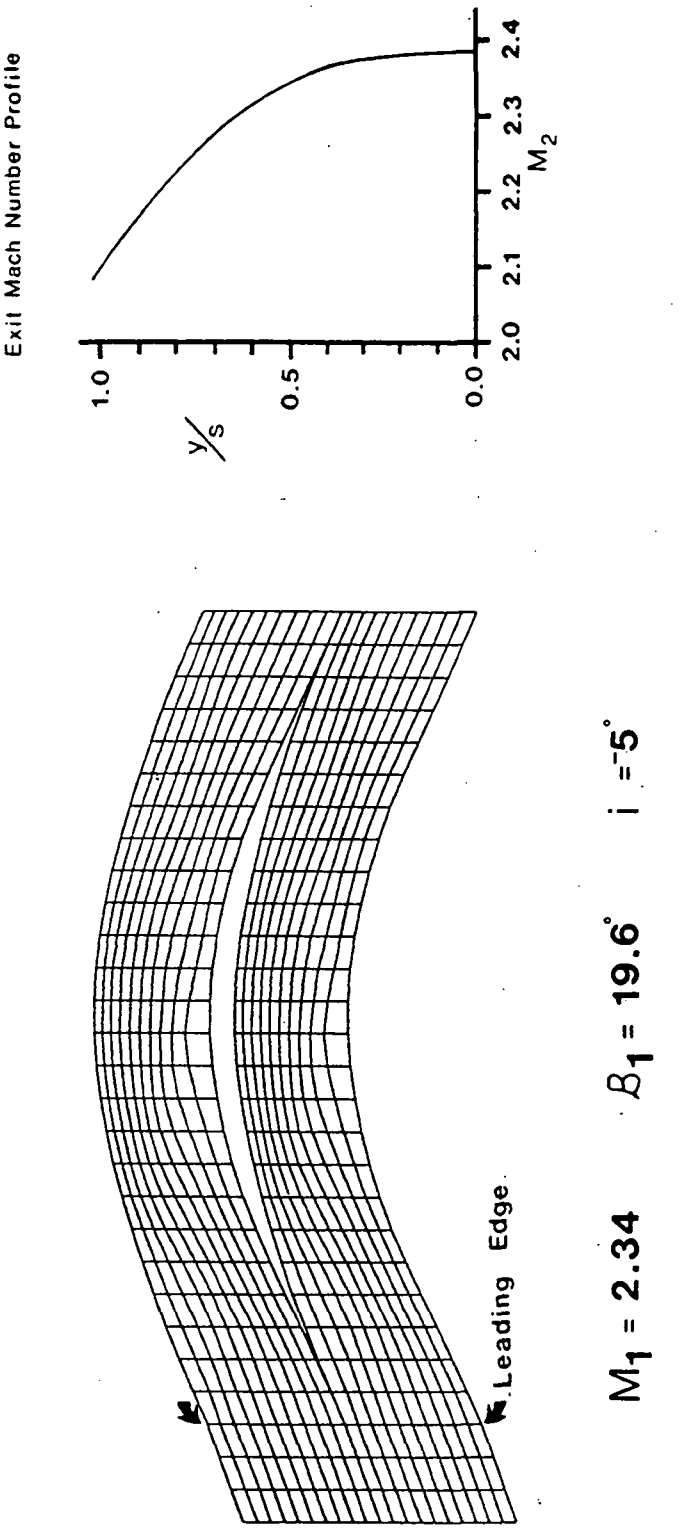

Figure 3.12 (cont.) Effect of incidence angle on flow in rotor cascade with axial Mach number 2.2.

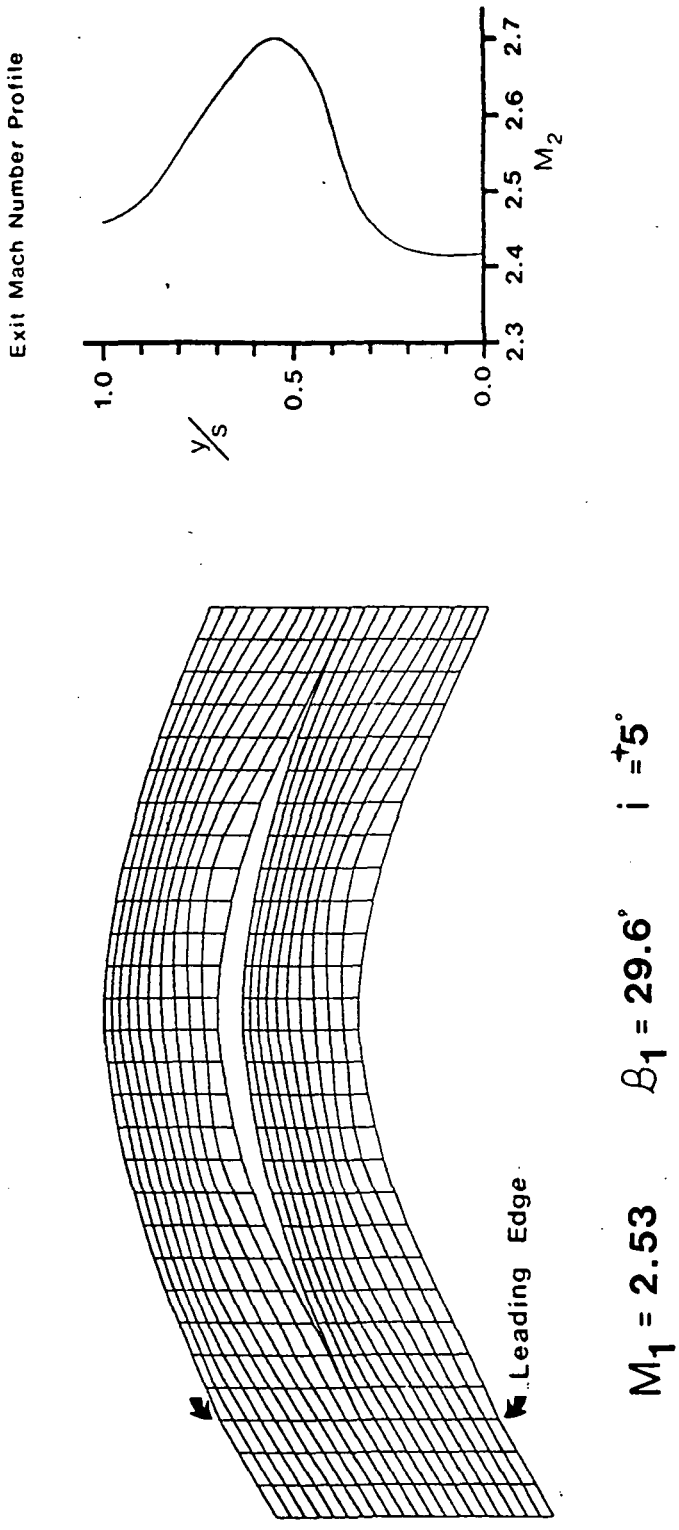

Figure 3.12 (cont.) Effect of incidence angle on flow in rotor cascade with axial Mach number 2.2.

non-uniformities in the rotor exit flow. This will likely lead to an increase in losses from rotor-stator interaction and greater noise.

3.6.4 VARIATION OF MACH NUMBER AT ROTOR DESIGN FLOW ANGLE

With the flow angle at the entrance to the rotor cascade held at the design value 24.6 degrees, the flow inlet Mach number was varied as an input to the supersonic Euler solver. Fully converged solutions were achieved down to an axial Mach number of 1.60, corresponding to a relative Mach number of 1.76. The Mach number was increased beyond the design value to an axial Mach number of 2.50 corresponding to a relative Mach number of 2.76. Streamline grids and exit Mach number profiles are shown in Figure 3.13.

For the cases studied, no shocks are perceptible from looking at the streamline grids. The exit Mach number profiles indicate flow non-uniformities similar in magnitude to those observed when the blade incidence angle was varied, and the implications are the same, increased losses and greater noise.

Since it was proposed in this investigation to operate in an axially supersonic condition down to a fan face Mach number of 1, loss of convergence of the Euler solver at axial Mach numbers below 1.60 is cause for some concern. Clearly, more work is required in this area, but this may indicate the necessity of variable geometry blades to maintain high relative Mach numbers as the axial Mach number is decreased.

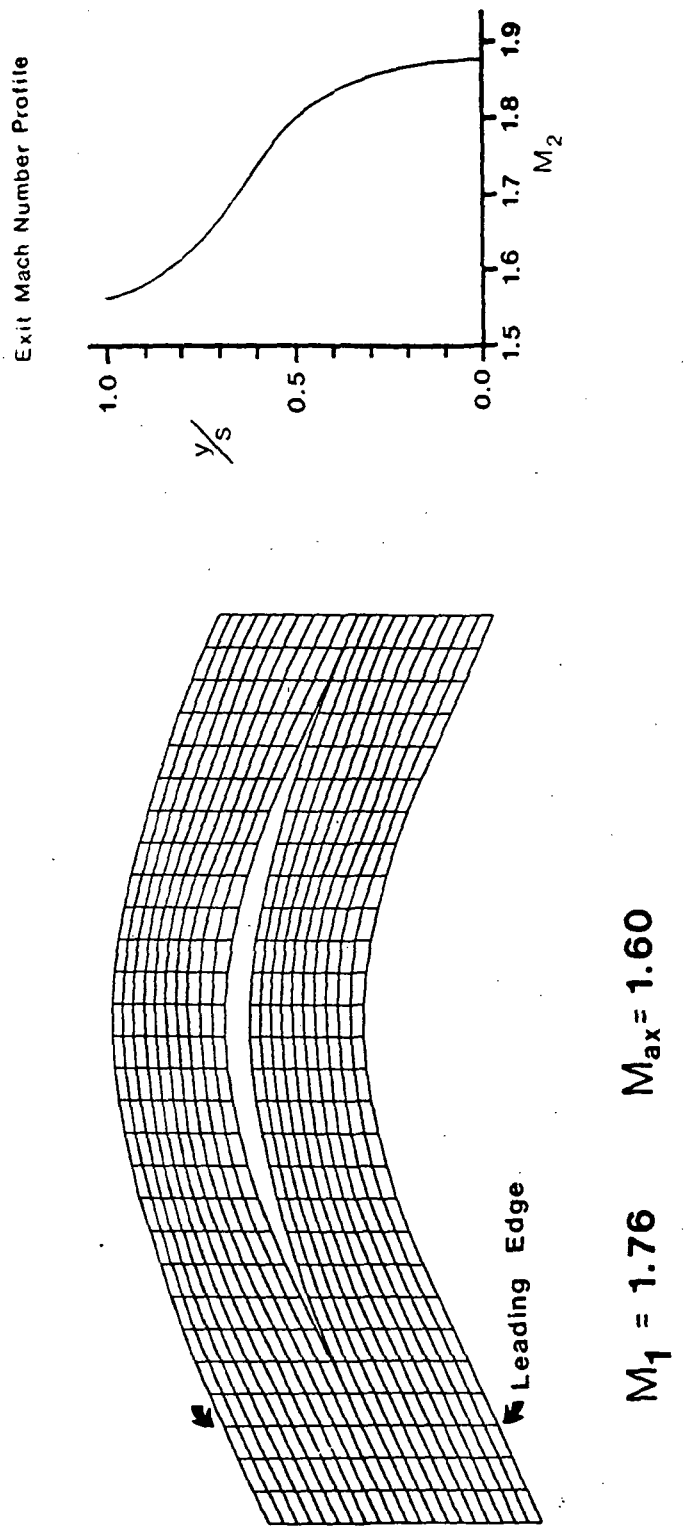

Figure 3.13 Effect of variation of Mach number on flow in rotor cascade at 24.6° design flow angle.

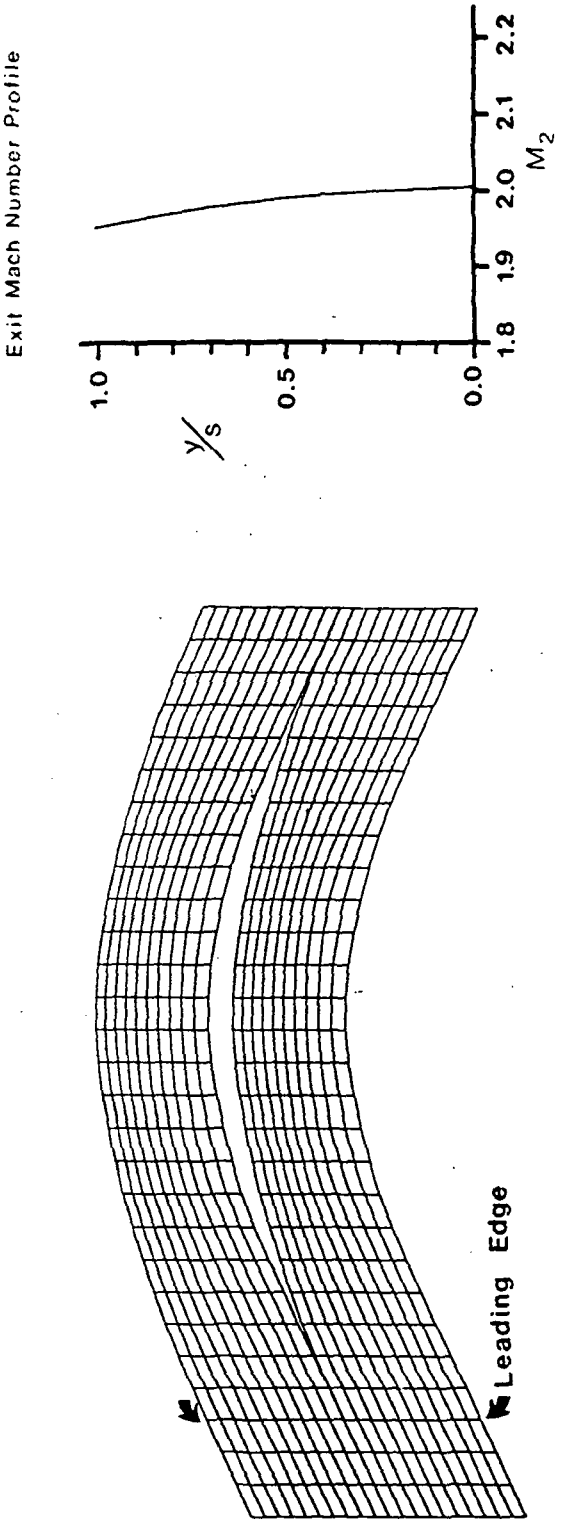

Figure 3.13 (cont.) Effect of variation of Mach number on flow in rotor cascade at 24.6° design flow angle.

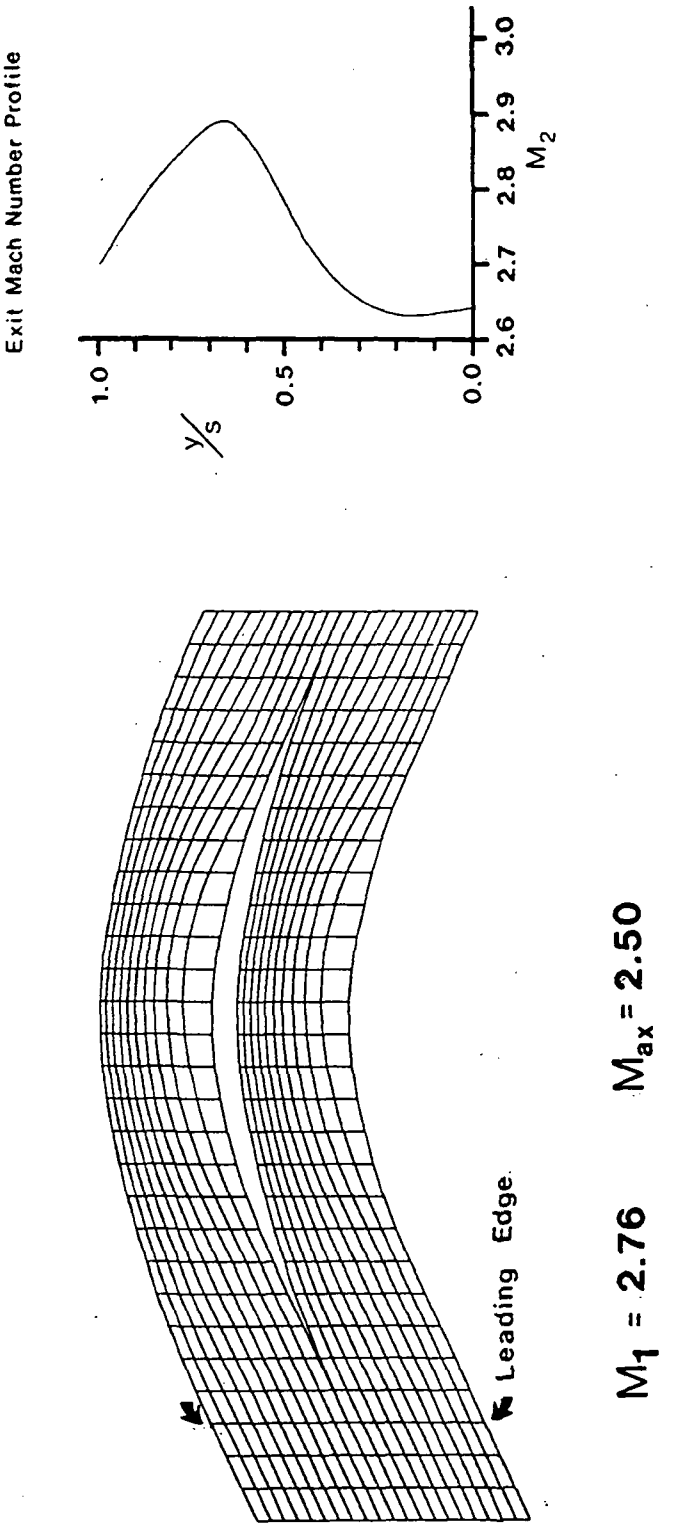

Figure 3.13 (cont.) Effect of variation of Mach number on flow in rotor cascade at 24.6° design flow angle.

C-2

3.7 SUMMARY OF WORK ON BLADING DESIGN AND RECOMMENDATIONS FOR FUTURE WORK

The work on the supersonic fan, while encouraging, also indicates a number of areas where more work is needed. The cascade designs presented herein suggest that at the design point good efficiency can be expected from the superflow fan. It was shown that the design goals of uniform exit flow, low passage diffusion factors, and minimal shocks within the passages can be achieved.

However, the concept requires further study. The performance of blades in anticipated off design conditions needs a great deal of exploration. Study of the range of incidence angles and Mach numbers over which fully supersonic flow can be maintained, and of the effects of the rotor on the flow in the stator must be undertaken. Even at the design condition, where it is expected that maintaining uniform flow at the rotor exit will cut down on unsteady shock losses, further analytical or experimental work is needed.

Some preliminary work suggests that variable rotor geometry or a rotor inlet guide vane may be required to avoid excessive blade incidence angles and maintain high fan pressure ratio at off design conditions. As pointed out in the section on loss calculation, the adverse effects of shock wave-boundary layer interaction have not been addressed in this study.

One fundamental point that must be worked on before the

axially supersonic fan can be considered a viable concept is the problem of attaining supersonic flow, or starting the flow through the stage. In the preceding sections, it has been assumed that supersonic flow can be achieved throughout the machine and that downstream conditions have no effect on the flow upstream. In order to achieve this condition, the blade passages must start in the same manner that a supersonic inlet must start. This is a more complicated problem for supersonic turbomachinery, since one blade row could interfere with the starting of another. An example of a potential difficulty might be a machine in which the rotor must start before being able to provide a high enough Mach number to start the stator, but the unstarted stator limits mass flow such that the rotor cannot start. The starting of single passages and isolated cascades is addressed in References 7 and 8, but a definitive study of starting an entire stage is clearly lacking.

4. CONCLUSION

The performance improvement offered by the superflow engine for a long range Mach 2.7 supersonic transport predicted in this study tends to support the results of previous work. The investigation performed on the aerodynamic design of the supersonic fan stage is encouraging in that good performance is predicted at the design point. Future study of the superflow fan concept should include work on off design performance and supersonic starting of the fan stage. Results of this work will be important in determining if the superflow fan is sufficiently versatile throughout the specified operating regime. While the challenges presented in the design of the superflow engine are indeed great, the potentially large benefits in performance justify further analytical and experimental research in this area.

References

1. Trucco, Horacio, "Study of Variable Cycle Engines Equipped with Supersonic Fans" ATL TR201, NASA CR-13477,September 1975.

2. Franciscus, Leo C., "Supersonic Through Flow Fan Engines for Supersonic Cruise Aircraft", NASA TM-78889,April 1978.

3. Kerrebrock, Jack L., Aircraft Engines and Gas Turbines. Cambridge, MA. The MIT Press, 1977.

4. Oates, Gordon C., "Non Ideal Cycle Analysis", Chapter 7 of The Aerothermodynamics of Aircraft Turbine Engines, G.Oates, Editor. AFAPL TR-78-52, 1978.

5. Moeckel, W.E., and Connors, J.F., "Charts for the Determination of Supersonic Flow Against Inclined Planes and Axially Symmetric Cones", NACA TN 1373, July 1947.

6. Kantrowitz, Arthur, "The Supersonic Axial Flow Compressor", NACA Report 974, 1950.

7. Ferri, Antonio, "Aerodynamic Properties of Supersonic Compressors", High Speed Aerodynamics and Jet Propulsion, Vol. 10. Princeton, N.J., 1964.

8. Boxer, Emanuel, Sterrett, James R., and Wlodarski John, "Application of Supersonic Vortex Flow Theory to the Design of Supersonic Impulse Compressor or Turbine Blade Sections", NACA RML52B06, 1952.

9. Goldman, Louis J., and Scullin, Vincent J., "Analytical Investigation of Supersonic Turbomachinery Blading, I. Computer Program for Blading Design", NASA TN D-4421, 1968.

10. Drela M., Giles M., and Thompkins, W.T. Jr., "Conservative Streamtube Solution of Steady State Euler Equations", AIAA-84-1643, 1984.

11. Breugelmans, F.A.E., "The Supersonic Axial Inlet Component in a Compressor," ASME 75-GT-26, 1975.

12. Breuglemans, F.A.E.,"High Speed Cascade Testing and Its Application to Axial Flow Supersonic Compressors," ASME 68-GT-10, 1968.

13. Lieblein, S., "Experimental Flow in Two-Dimensional Cascades," Aerodynamic Design of Axial Flow Compressors, NASA SP-36, 1965.

14. Tipton, D.L., "Improved Techniques for Compressor Loss Calculation," Allison Division General Motors Corporation.

APPENDIX A. SUMMARY OF METHODS USED IN CYCLE ANALYSIS

The cycle analysis was carried out using methods of quantitive cycle analysis as outlined in references 3 and 4. A simple FORTRAN program was developed to permit quick cycle calculations. A listing of this is included. The engine stations and basic equations are as follows:

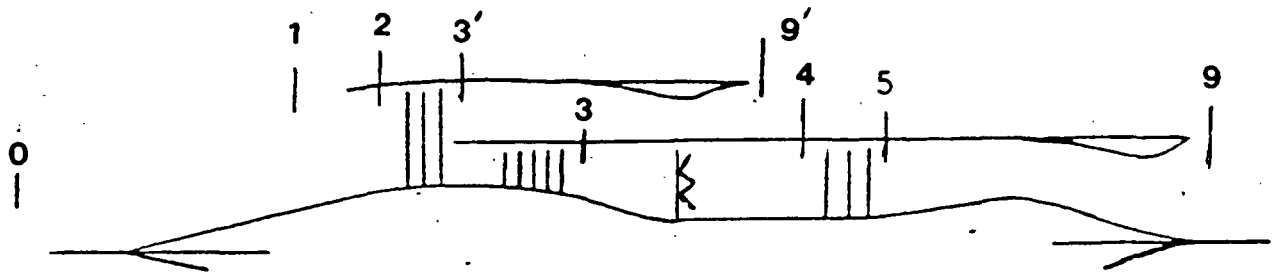

Figure A1. Schematic of Engine Stations

For a dry turbofan with nozzle expansion to p_0 specific thrust is given by:

$$\frac{F}{\dot{m}a_0} = \left\{(1+f)\left(M_0 \frac{U_9}{U_0}\right) - M_0 + \alpha\left(M_0 \frac{U_9'}{U_0} - M_0\right)\right\}$$

and specific impulse is:

$$I = \frac{F}{\dot{m}_f g} = \frac{F}{\dot{m}a_0}\left(\frac{a_0}{fg}\right)$$

where:

$$M_0 \frac{U_9}{U_0} = \left[\frac{2}{\gamma_c - 1}\theta_t \tau_t \left\{1 - \left(\frac{p_{t9}}{p_0}\right)^{-\left(\frac{\gamma_t - 1}{\gamma_t}\right)}\right\}\right]^{1/2}$$

and:

$$M_0 \frac{U_9'}{U_0} = \left[\frac{2}{\gamma_c - 1}\theta_0 \tau_c' \left\{1 - \left(\frac{p_{t9}'}{p_0}\right)^{-\left(\frac{\gamma_c - 1}{\gamma_c}\right)}\right]^{1/2}$$

$$\frac{P_{tq}}{P_0} = \delta_0 \pi_d \pi_c \pi_b \pi_t \pi_n \qquad \frac{P'_{tq}}{P_0} = \delta_0 \pi_d' \pi_c' \pi_n'$$

The total temperature ratio across the turbine τ_t is given by:

$$\tau_t = 1 - \frac{1}{\eta_m (1+f)} \frac{\theta_0}{\theta_t} \left[(\tau_c - 1) + \alpha (\tau_c' - 1) \right] \frac{C_{pc}}{C_{pt}}$$

The fuel to mass flow ratio is given by:

$$f = \frac{\dot{m}_f}{\dot{m}} = \left\{ \frac{\theta_t - \theta_0 \tau_c}{\frac{h \eta_b}{C_{pc} T_0} - \theta_t} \right\}$$

Pressure and temperature ratios in the various rotating components are related through their polytropic efficiencies by the formulae:

For Compressor: $\tau_c = \pi_c^{\left(\frac{\gamma_c - 1}{\gamma_c e_c}\right)}$

Fan: $\tau_c' = \pi_c'^{\left(\frac{\gamma_c - 1}{\gamma_c e_c'}\right)}$

Turbine: $\pi_t = \tau_t^{\left(\frac{\gamma_t}{(\gamma_t - 1) e_t}\right)}$

The ratio of constant pressure specific heats between compressor and turbine is given by:

$$\frac{C_{pc}}{C_{pt}} = \frac{\gamma_c}{(\gamma_c - 1)} \frac{(\gamma_t - 1)}{\gamma_t}$$

Symbols Used in Cycle Analysis

T_0	Ambient temperature
γ_c	Ratio of specific heats (compressor or fan)
γ_t	Ratio of specific heats in turbine
C_{pc}	Constant pressure specific heat, compressor
C_{pt}	Constant pressure specific heat, turbine
h	Heat value of fuel
π_d	Pressure ratio in diffusing from free stream to core compressor
π_d'	Pressure ratio in diffusing from free stream to fan face
π_b	Pressure ratio across burner
π_n'	Pressure ratio across fan nozzle
π_n	Pressure ratio across core nozzle
η_b	Burner efficiency
e_c	Polytropic efficiency in compression of core flow from diffuser exit to compressor exit
e_c'	Polytropic efficiency of fan
e_t	Polytropic efficiency of turbine
θ_t	Ratio of turbine inlet temperature to free stream temperature ratio
π_c	Compression ratio of core flow
π_c'	Compression ratio of fan flow
α	Bypass ratio
δ_0	Ratio of total to static pressure in free stream
θ_0	Ratio of total to static temperature in free stream
η_m	Fuel/Air mixing efficiency (Set to 1)
g	Acceleration of gravity
$\dot{m}$	Mass flow through core

PERFOR.FOR;10

```
      C       INTERACTIVE INPUT OF FLIGHT CONDITIONS
0001   10     TYPE*, ' TYPE 1 TO CHANGE FLIGHT CONDITIONS '
0002          ACCEPT*, IFC
0003          IF (IFC.EQ.1) THEN
0004          TYPE*, 'INPUT THE FLIGHT MACH NUMBER '
0005          ACCEPT*, FM
0006          THETA = 1 + 0.2*(FM**2)
0007          DEL = (THETA)**3.5
0008          TYPE*, 'INPUT THE AMBIENT TEMPERATURE IN DEGREES RANKINE'
0009          ACCEPT*, T0
0010          ELSE
0011          ENDIF
      C       ---------------------
      C       INTERACTIVE INPUT OF ENGINE VARIABLES
0012          TYPE*, 'TYPE 1 TO CHANGE ENGINE VARIABLES '
0013          ACCEPT*, IEV
0014          IF (IEV.EQ.1) THEN
0015          TYPE*, ' INPUT THE TOTAL PRESS. ACROSS FAN DIFFUSER '
0016          ACCEPT*, PIDF
0017          TYPE*, ' INPUT THE TOTAL PRESS. ACROSS CORE DIFFUSER '
0018          ACCEPT*, PIDC
0019          TYPE*, ' INPUT THE TOTAL PRESSURE RISE IN THE CORE '
0020          ACCEPT*, PIC
0021          TYPE*, ' INPUT THE TOTAL PRESSURE RISE IN THE FAN '
0022          ACCEPT*, PIF
0023          TYPE*, ' INPUT COMPRESSOR POLYTROPIC EFFICIENCY '
0024          ACCEPT*, EC
0025          TYPE*, ' INPUT FAN POLYTROPIC EFFICIENCY '
0026          ACCEPT*, EF
0027          TYPE*, ' INPUT TURBINE POLYTROPIC EFFICIENCY '
0028          ACCEPT*, ET
0029          TYPE*, ' INPUT THE TURBINE INLET TEMPERATURE IN RANKINE '
0030          ACCEPT*, TTI
0031          THET4 = TTI/T0
0032          TYPE*, ' INPUT THE BYPASS RATIO '
0033          ACCEPT*, BPR
0034          TYPE*, ' INPUT THE PRESSURE RATIO ACROSS THE BURNER '
0035          ACCEPT*,PIB
0036          TYPE*, ' INPUT THE BURNER EFFICIENCY '
0037          ACCEPT*, ETAB
0038          TYPE*, ' INPUT THE PRESSURE RATIO ACROSS THE CORE NOZZLE'
0039          ACCEPT*, PINC
0040          TYPE*, ' INPUT THE PRESSURE RATIO ACROSS THE FAN NOZZLE'
0041          ACCEPT*, PINF
0042          ELSE
0043          ENDIF
      C       ---------------------
      C       SPECIFIC THRUST CALCULATION
0044          GAMC = 1.40
0045          GAMT = 1.333
0046          TAUC = PIC**((GAMC-1)/(GAMC*EC))
0047          TAUF = PIF**((GAMC-1)/(GAMC*EF))
0048          H = 19000
0049          CPC = 0.240
0050          F = (THET4-(THETA*TAUC))/((H*ETAB/(CPC*T0))-THET4)
```

PERFOR.FOR;10

```
0051            SHR = (GAMC*(GAMT-1))/(GAMT*(GAMC-1))
0052            ETAM = 1
0053            TAUT = 1 - (1/(ETAM*(1+F)))*(THETA/THET4)*
               1 ((TAUC-1)+BPR*(TAUF-1))*SHR
0054            PIT = TAUT**(GAMT/((GAMT-1)*ET))
0055            P9C = DEL*PIDC*PIC*PIB*PIT*PINC
0056            P9F = DEL*PIDF*PIF*PINF
0057            FMU9C = ((2/(GAMC-1))*THET4*TAUT*
               2  (1-P9C**((1-GAMT)/GAMT)))**0.5
0058            FMU9F = ((2/(GAMC-1))*THETA*TAUF*
               3  (1-P9F**((1-GAMC)/GAMC)))**0.5
0059            FSPEC = ( (1+F)*FMU9C-FM+BPR*(FMU9F-FM))
        C       ----------------
        C       OUTPUT OF RESULTS AND OPTION TO RUN AGAIN
0060            TYPE*, ' TURBINE TEMP RATIO IS',TAUT
0061            TYPE*, ' SPECIFIC THRUST IS ',FSPEC
0062            TYPE*, ' FMU9C IS ',FMU9C
0063            TYPE*, ' FMU9F IS ',FMU9F
0064            TYPE*, ' F IS ',F
0065            TYPE*, ' PRESS 1 TO RUN AGAIN '
0066            ACCEPT*, IRA
0067            IF (IRA.EQ.1) THEN
0068            GOTO 10
0069            ELSE
0070            ENDIF
0071            END
```